funded by the European Union

Awareness and resilience through European multi sensor system

D2.2– GIS map and database of geology and seismotectonics of the selected areas

Version 1 15/05/2023

Disclaimer

Document type	Deliverable
Document number	D2.2 version 1
Document title	GIS map and database of geology and seismotectonics of the selected areas
Authors	Michele Carafa, Gaetano De Luca, Deborah Di Naccio, Vassileios Karakostas, Christos Kourouklas, Eleftheria Papadimitriou, Alessandra Sciortino, Stylianos Stoulos, Michael Strupler, Marco Tallini
Release date	15/05/2023
Contributing partners	AuTh, ETH, INGV, UNIVAQ
Dissemination level	Public

Version	Short description	Main authors	Coordinator
1	First release	Michele Carafa, INGV Gaetano De Luca, INGV Deborah Di Naccio, INGV Vassileios Karakostas, AuTh Christos Kourouklas, AuTh Eleftheria Papadimitriou, AuTh Alessandra Sciortino, UNIVAQ Stylianos Stoulos, AuTh Michael Strupler, ETH Marco Tallini, UNIVAQ 15.5.2023	Ayse Nyberg, KTH

Abstract

The present deliverable regards the description of the database and maps stored into the GIS project concerning on the geology and seismotectonics of the three areas selected within the artEmis project (Abruzzi region, Italy; Ionian islands and the Gulf of Corinth, Greece; Bedretto lab and Swiss Alps).

The potential groundwater sites for radon monitoring will be chosen within the three areas.

The Abruzzi region (Italy) has been managed by UNIVAQ and INGV, the Ionian islands and the Gulf of Corinth (Greece) by AUTh, and Bedretto lab and Swiss Alps by ETH.

The interplay of the geological and seismotectonic data with the other geoscience ones (hydrogeology, and seismicity) will permit to better locate the potential radon monitoring sites.

Table of contents

1 Introduction

The present deliverable regards the description of database and maps stored into the GIS project concerning the geology and seismotectonics of the three areas selected within the artEmis project (Abruzzi region, Italy; Ionian islands and the Gulf of Corinth, Greece; Bedretto lab and Swiss Alps) (fig. 1.1).

The potential groundwater sites for radon monitoring will be chosen within the three areas.

The Abruzzi region (Italy) has been managed by UNIVAQ and INGV, the Ionian islands and the Gulf of Corinth (Greece) by AUTh, and Bedretto lab and Swiss Alps by ETH.

The interplay of the geological and seismotectonic data with the other geoscience ones (hydrogeology, and seismicity) will permit to better locate the potential radon monitoring sites.

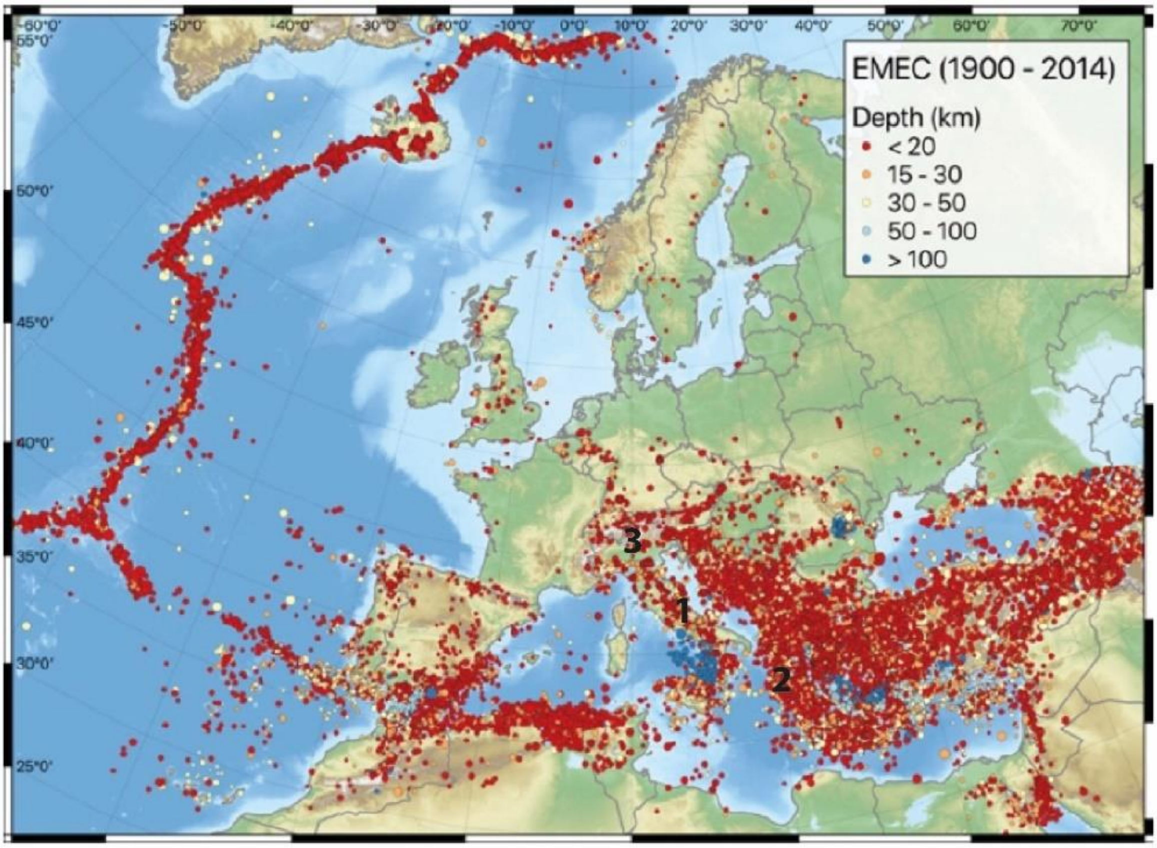

Figure 1.1: The complete European-Mediterranean earthquake catalogue (EMEC) for the period 1900 – 2012 by Danciu et al. (2021) with the location of the three selected areas (1: Abruzzi region, Italy; 2: Ionian Islands and Gulph of Corinth, Greece; 3: Bedretto lab and Swiss Alps)

1.1 References

Danciu, L., Nandan, S., Reyes, C., Basili, R., Weatherill, G., Beauval, C., Rovida, A., Vilanova, S., Sesetyan, K., Bard, P-Y., Cotton F., Wiemer, S., Giardini, D., 2021. The 2020 update of the European Seismic Hazard Model: Model Overview. EFEHR Technical Report 001, v1.0.0. https://doi.org/10.12686/a15

2 GIS map and database of geology and seismotectonics (Abruzzi region, Italy)

For selecting the potential groundwater sites for radon monitoring a GIS map and database was organised. The free and open-source Geographic Information System QGIS (https://qgis.org/en/site/) was used.

The QGIS project is available at the Department of Civil, Architectural and Environmental Engineering of L'Aquila University (UNIVAQ).

In the QGIS project of Abruzzi region several geoscience informative database and maps concerning geology, seismotectonics, seismicity and hydrogeology, were stored and divided into three main folders:

Deliverable 2.2 – Geology and seismotectonics;

Deliverable 2.4 – Seismicity;

Deliverable 2.6 – Hydrogeology.

In this deliverable (D2.2) the maps and database of geology and seismotectonics stored in the QGIS project are described, while, in the deliverables D2.4 and D2.6 the geoscience data stored in the QGIS project concerning the seismicity and hydrogeology are outlined respectively.

The geological and seismotectonic data and maps stored in the QGIS project are organized as shown in figure 2.1.

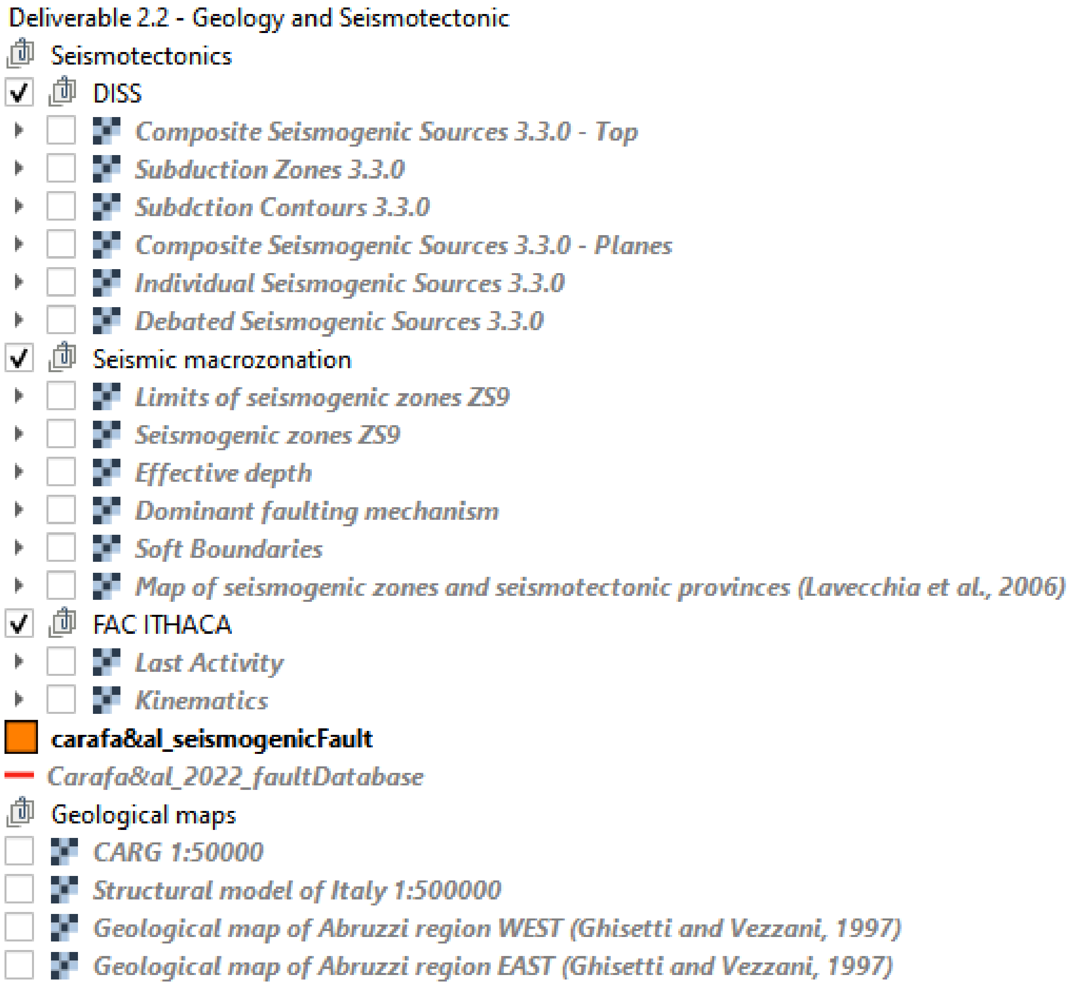

Figure 2.1: Geological and seismotectonic data and maps organised in the QGIS project

Moreover, the location of the potential groundwater sites for radon monitoring was stored too. They are mainly wells and springs managed by the Water Management Companies of Abruzzi region (tab. 2.1) and specific sites managed by INGV (fig. 2.2).

Further, the GIS project is enriched by various cartographic basemap such as Google Maps, regional DEM (Digital Elevation Model) with a resolution of 10 m, cadastral maps, and regional and municipal boundaries (fig. 2.3).

WMC	ADP
ACA	Pescara District
GSA	L'Aquila District
RUZZO	Teramo District
CAM	Avezzano area (L'Aquila District)
SACA	Sulmona area (L'Aquila District)
SASI	Chieti District

Table 2.1: the Water Management Companies (WMC) of Abruzzi region and their relative areas of competence (Administrative District Province and main towns: ADP)

The QGIS project permits to overlap the different geoscience data and maps with the potential groundwater sites for radon monitoring, so to facilitate the selection of the latter ones.

As an example, the QGIS project allows to identify the potential sites closer to the active seismogenic faults which are considered, in a conceptual model, an important feature for the radon upwelling from the earthquake focus considered the initial seismic rupture zone (figs. 2,3, 2.4).

The more interesting sites within the artEmis project are those placed along the Apennines chain (L'Aquila district) which is an area with high values of PGA (Peak Ground Acceleration) and where several seismogenic faults are located. Conversely, in the Adriatic coastal area doES not present the seismogenic faults and is characterised by lower PGA values (figs. 2.3, 2.4).

Moreover, in the Abruzzi region the significant areas to select the potential sites are the large intermontane plains, such as L'Aquila, Fucino, and Sulmona, and the Val Roveto valley. These areas are encircled by significant seismogenic faults (e.g. for L'Aquila: Pizzoli and Paganica faults, for Fucino: Serrone and Trasacco faults, for Sulmona: Morrone Mt. fault, Val Roveto: Val Roveto fault) (Carafa et al., 2022) and in them wells and high discharge springs (e.g. for L'Aquila: Vetoio, Boschetto, Tempera and Capovera springs, for Fucino: Celano, Ferriera and Pulciara springs, for Sulmona: Giardino, Capopescara, San Calisto springs, Val Roveto: Liri, Rio Sonno, Verrecchie springs) are widespread (Boni et al., 1986; Celico, 1983) (figs. 2.5, 2.6). Further in these plains the epicentral areas of high magnitude (M>6) historical earthquakes are located (for L'Aquila: April 6, 2009 - Mw: 6.3 and February 2, 1703 – Mw: 6.7; for Fucino: January 13, 1915 – Mw: 7.0; for Sulmona: November 3, 1706 – Mw: 6.6). These plains represent also the most inhabited areas of the Apennine Abruzzo (i.e. L'Aquila district, the residents of L'Aquila district are about 300,000, the 25% of the whole Abruzzi) showing so a considerable seismic risk.

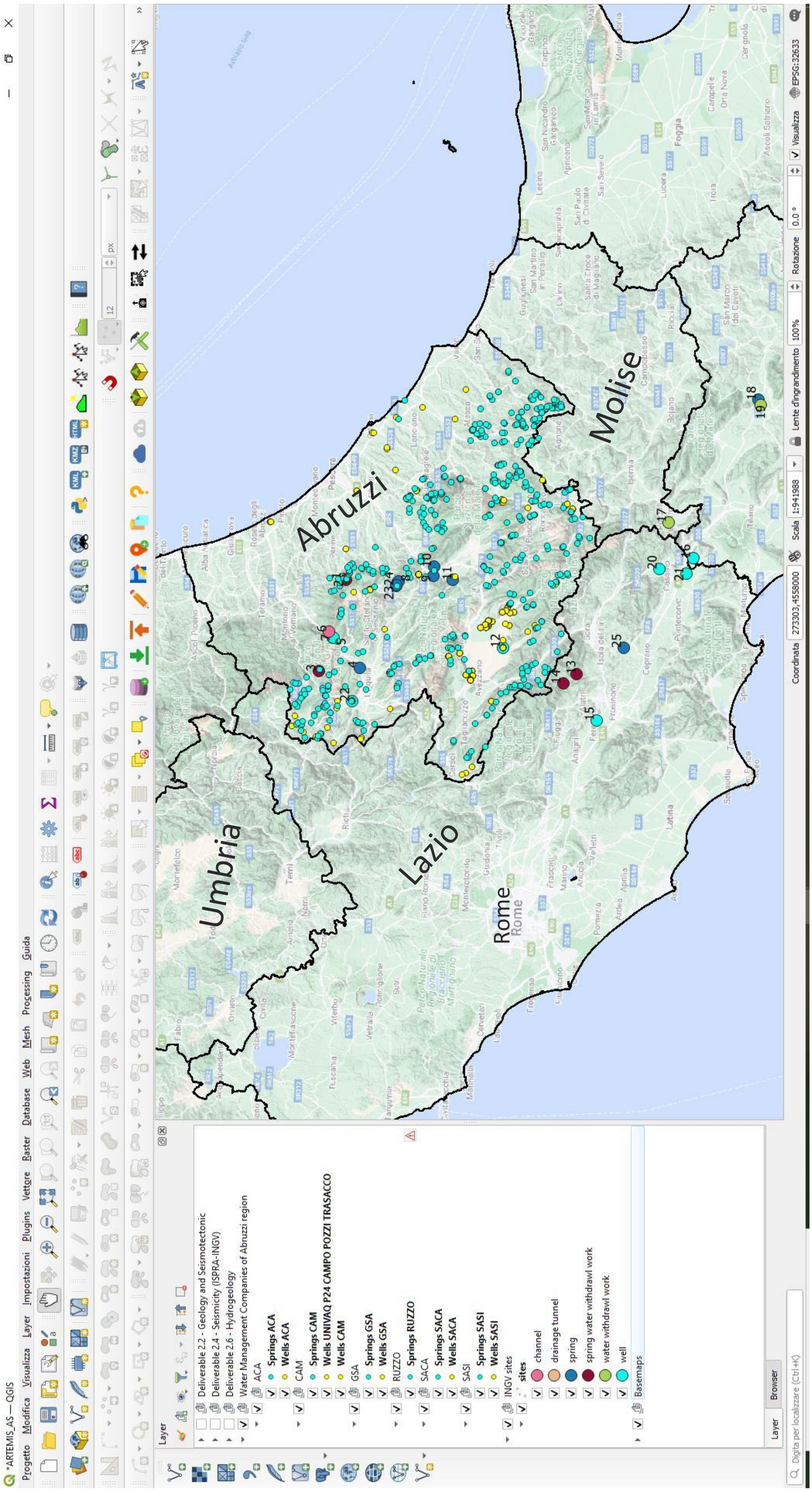

Figure 2.2: The structure of the QGIS project with the location of the potential sites, represented by wells (yellow) and springs (blue), of the Abruzzi Water Companies and specific sites managed by INGV

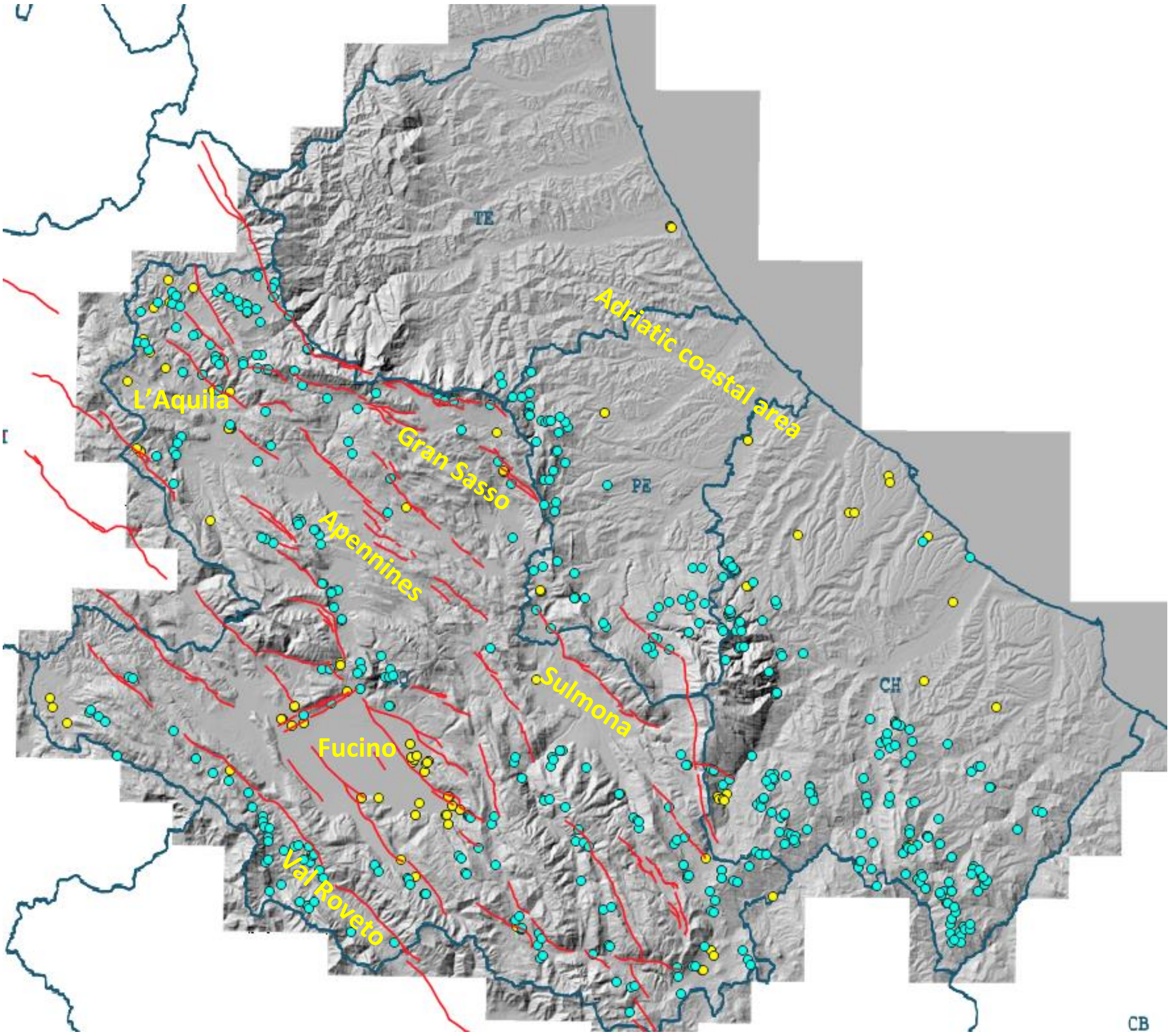

Figure 2.3: The potential sites for radon monitoring represented by wells (in yellow) and springs (in blue), of the Abruzzi Water Companies with the Digital elevation Model and the seismogenic faults from INGV database by Carafa et al. (2022)

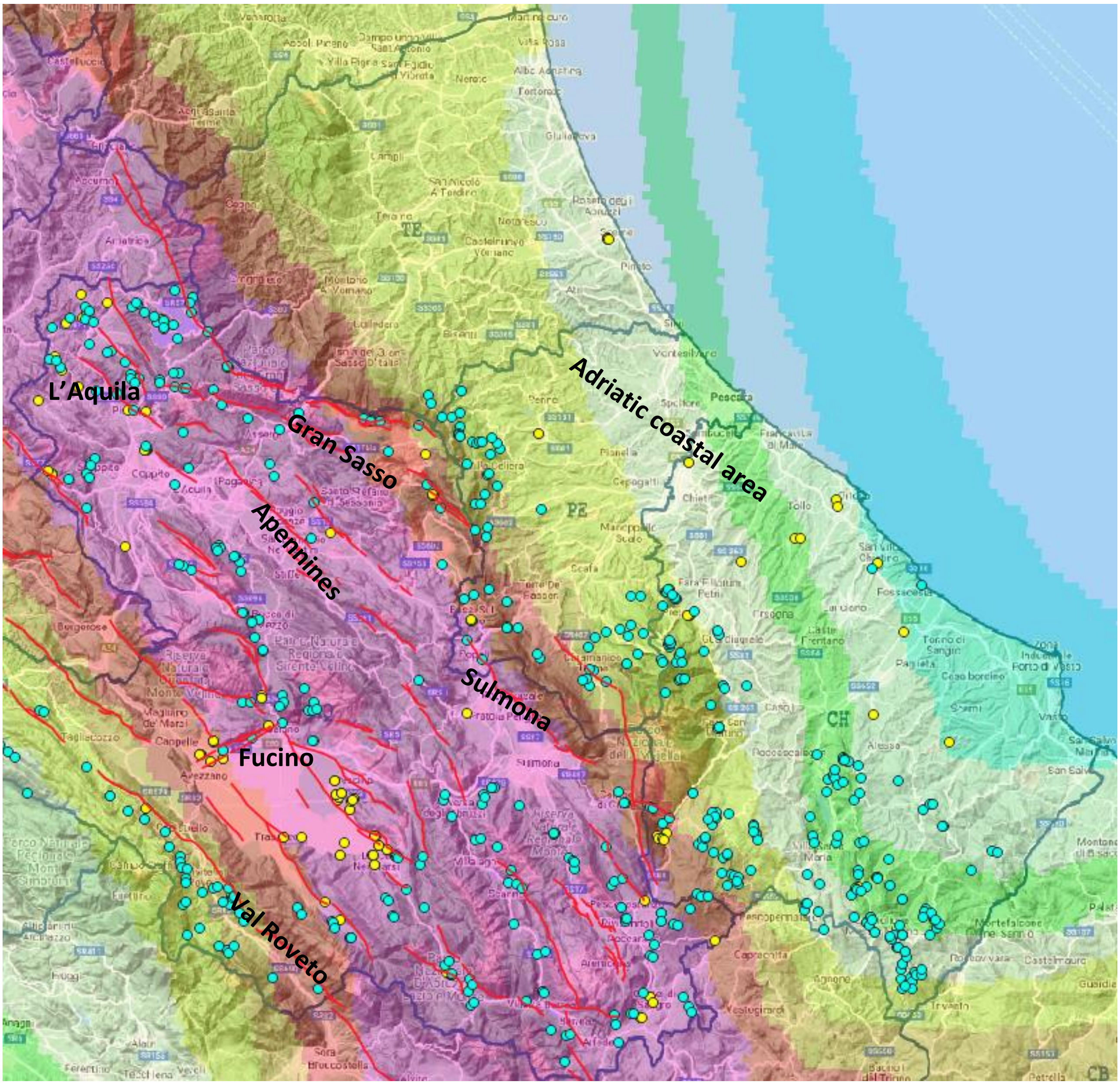

Figure 2.4: The potential sites (wells in yellow and springs in blue), of the Abruzzi Water Companies with the Digital elevation Model, the seismogenic faults by Carafa et al. (2022) and Peak Ground Acceleration (PGA). The higher and lower PGA values are red-violet and yellow-green colours, respectively

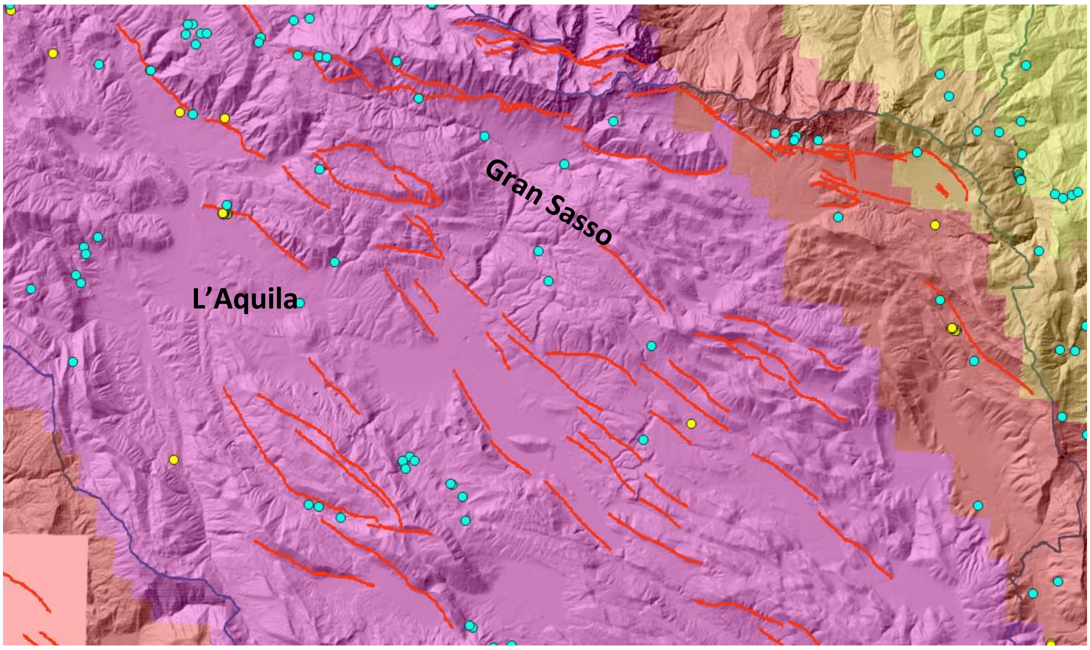

Figure 2.5: The potential sites (wells in yellow and springs in blue), of the Abruzzi Water Companies and the seismogenic faults and Peak Ground Acceleration (PGA) for L'Aquila area and Gran Sasso. The higher and lower PGA values are red-violet and yellow-green colours, respectively

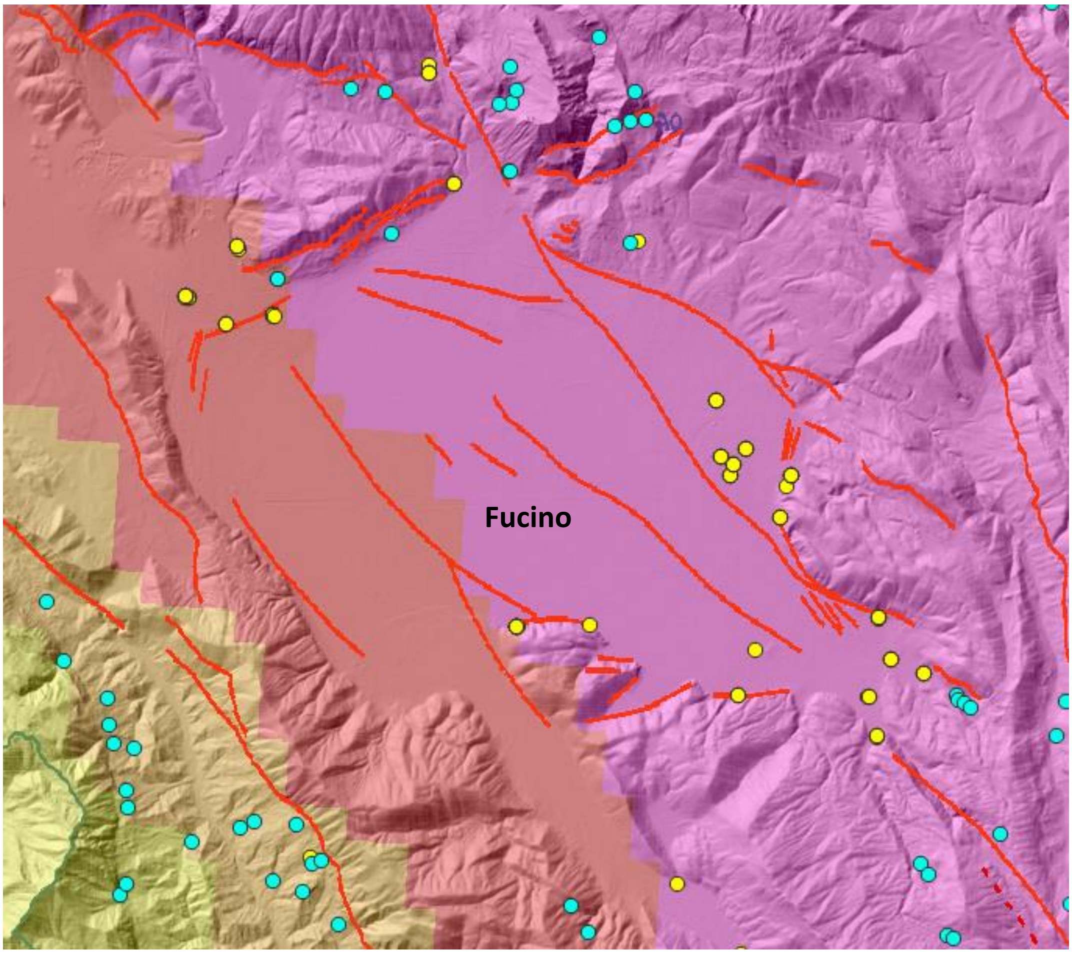

Figure 2.6: The potential sites (wells in yellow and springs in blue), of the Abruzzi Water Companies and the seismogenic faults and Peak Ground Acceleration (PGA) for the Fucino intermontane plain. The higher and lower PGA values are red-violet and yellow-green colours, respectively

2.1 Geological maps

The “Geological maps” folder contains the following maps at different scales (1:50,000, 1:100,000 and 1:500,000) (fig. 2.1):

the Italian geological maps at 1:50,000 scale of the CARG project, inserted in the QGIS project through WMS (URL: http://sgi2.isprambiente.it/arcgis/services/raster/geo_50k_italia/ImageServer/WMSServer) (Geological Survey of Italy, 2023);

the Geological map of Abruzzi by Vezzani and Ghisetti (1998) at 100,000 scale inserted in the QGIS project as georeferenced map;

The Structural model of Italy (sheet 4) by Bigi et al. (1992) at 1:500,000 scale as georeferenced map.

Basic knowledge of regional geology, integrated with other geoscience data, is essential to choose the better sites for the radon monitoring in the Abruzzi region. As an example, in the figures 2.7-2.10 the geological map by Vezzani and Ghisetti (1998) and by Bigi et al. (1992) are reported with the wells and springs of the Water Companies and the active faults by Carafa et al., (2022).

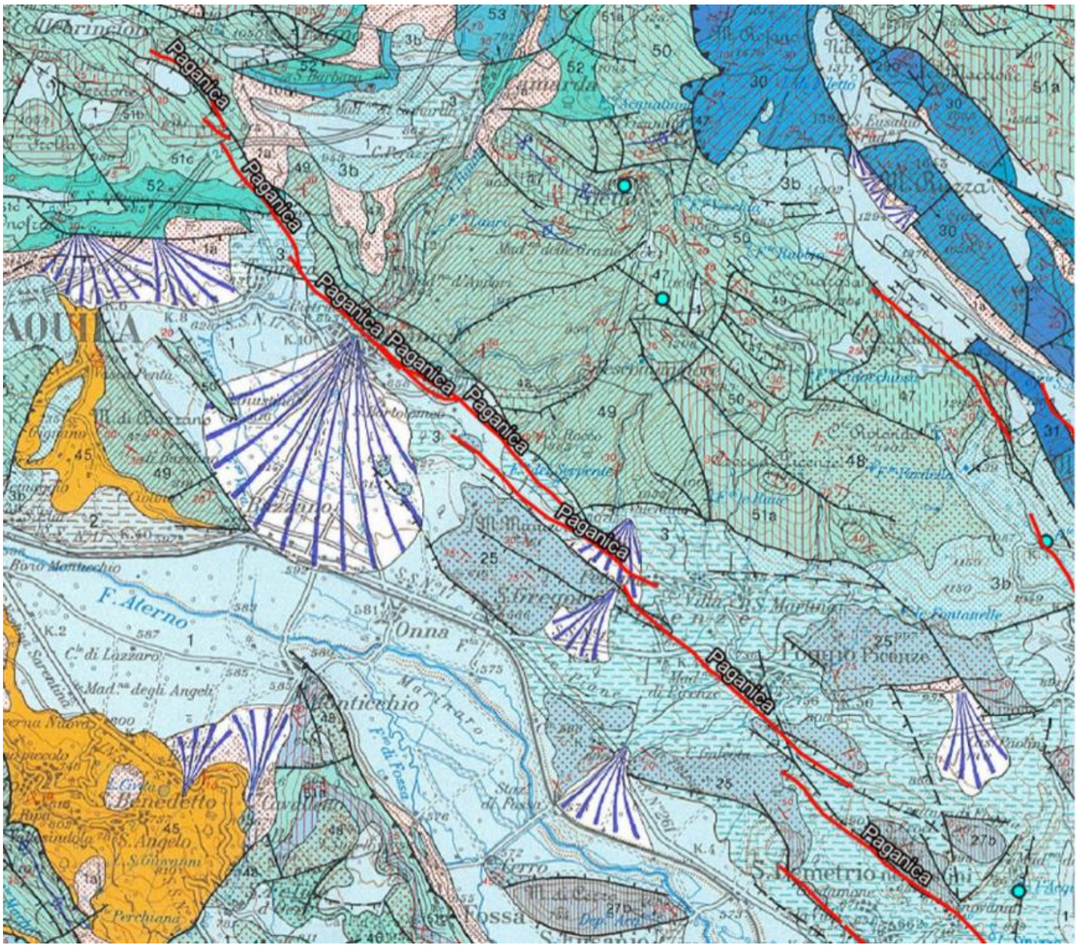

Figure 2.7: L’Aquila plain and the Paganica active fault: the active faults by Carafa et al. (2022) and the geological map of Abruzzi by Vezzani and Ghisetti (1998) at 1:100000 scale with the location of the potential radon monitoring sites (spring: blue dot, well: yellow dot)

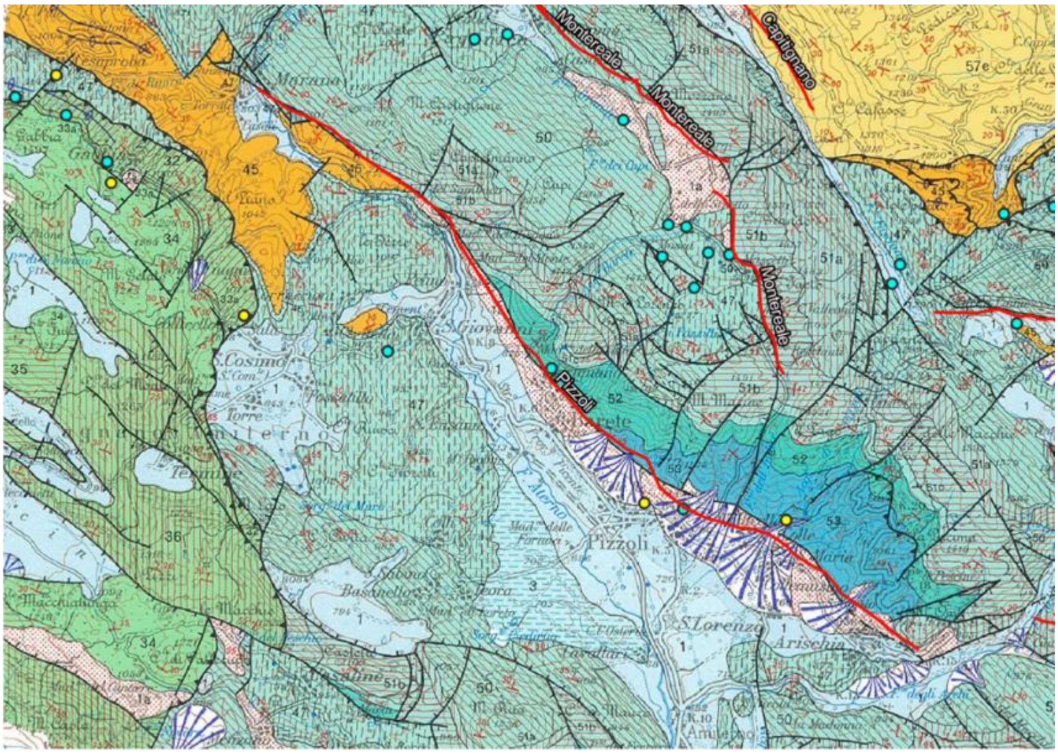

Figure 2.8: L'Aquila plain and the Pizzoli active fault: the active faults by Carafa et al. (2022) and the geological map of Abruzzi by Vezzani and Ghisetti (1998) at 1:100000 scale with the location of the potential radon monitoring sites (spring: blue dot, well: yellow dot)

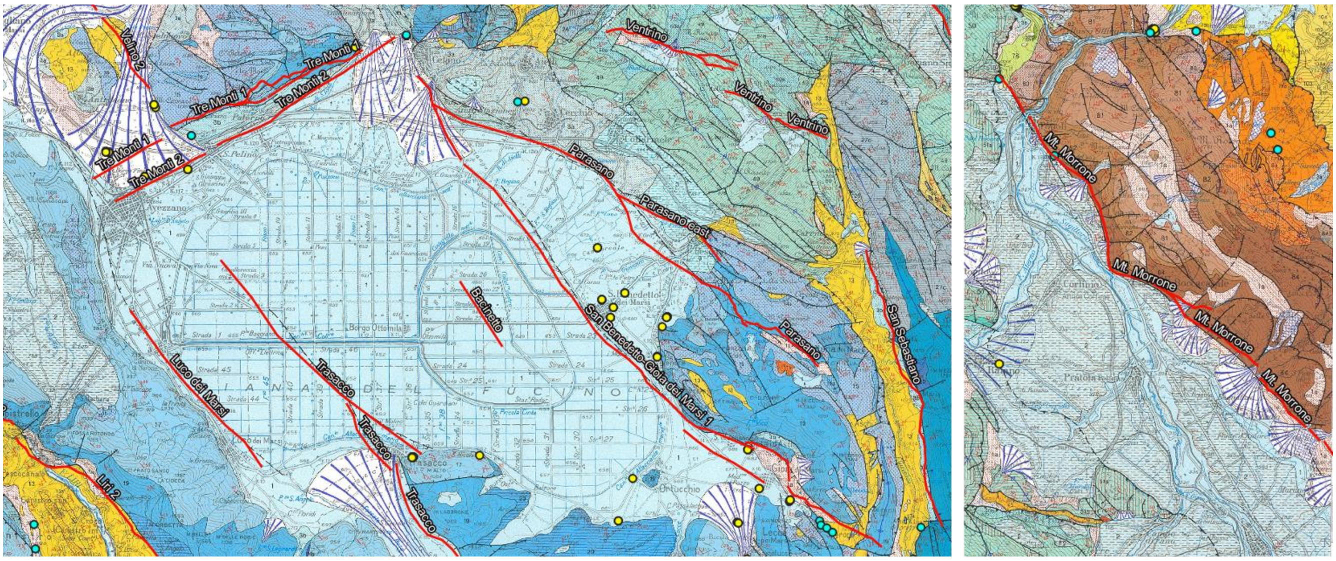

Figure 2.9: Fucino plain (left) and Sulmona plain (right): the active faults by Carafa et al. (2022) and the geological map of Abruzzi by Vezzani and Ghisetti (1998) at 1:100000 scale with the location of the potential radon monitoring sites (spring: blue dot, well: yellow dot)

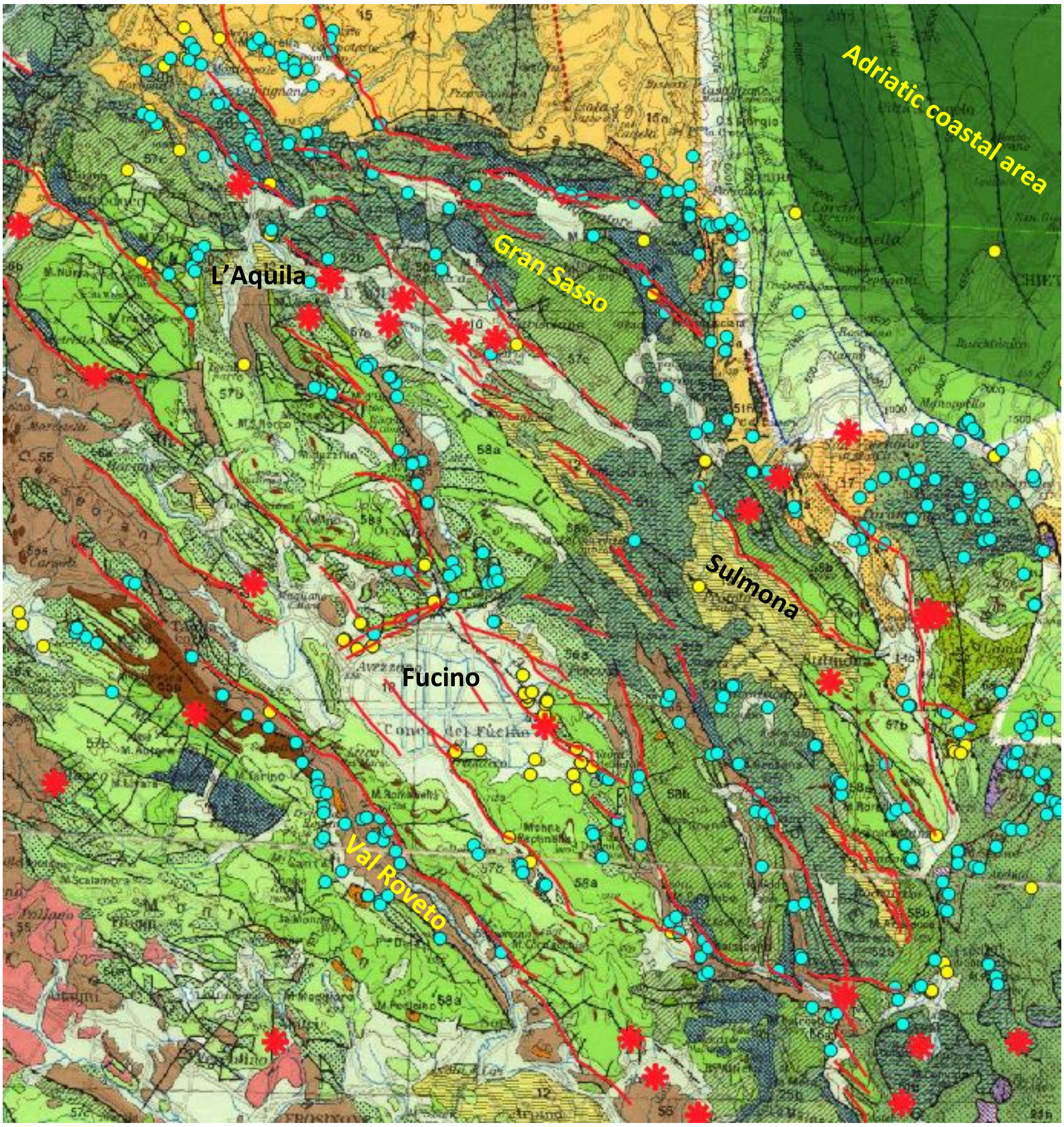

Figure 2.10: Zoom in of the Structural model of Italy (sheet 4) for the Abruzzi region (Bigi et al., 1992) with the location of the potential monitoring sites (blue dot: spring, yellow dot: well), the active faults by Carafa et al. (2022) and the main earthquakes by Guidoboni et al. (2018)

2.2 Seismotectonics

The “Seismotectonics” folder contains many information acquired from different sources and cataloged in three folders (fig. 2.1):

“DISS”;

“Seismic macrozonation”;

“FAC ITHACA”.

Within the above-mentioned folder the active faults, seismogenic sources, and seismogenic zones are stored. So here a brief definition of this elements. The active fault is a fault that is likely to become the source of another earthquake sometime in the future. Italian paleoseismologists commonly consider faults to be active if there has been coseismic rupture observed or evidence of seismic activity during the last 40,000 years (lower limit of radiocarbon dating). The radicarbon dating is used to date the soils involved in the surface rupture of the active fault.

The seismogenic source corresponds to Individual faults, or systems of faults, for which it is possible to calculate both the expected maximum earthquake magnitude and the ratio between the number of strong and weak earthquakes.

The seismogenic zone is a portion of the earth's crust or mantle from which earthquakes can originate. These elements, together with the earthquake catalogs and the seismic wave propagation models, are necessary to proceed with the probabilistic calculation of the seismic hazard and to classify the territory with respect to the seismic hazard.

2.2.1 Database of Individual Seismogenic Source (DISS)

The “DISS” (Database of Individual Seismogenic Source) folder contains the DISS version 3.3.0 by INGV which is a georeferenced repository of tectonic, fault, and paleoseismological data. It is an ensemble of potential sources for earthquakes larger than M 5.5 in Italy (https://diss.ingv.it/diss330/dissmap.html URL: https://services.seismofaults.eu/geoserver/DISS330/wms?request=getCapabilities) (DISS Working Group, 2021) (fig. 2.11). It is considered the magnitude 5.5 because usually it is assumed as the threshold value beyond which the fault responsible for the earthquake assumes such dimensions that it can be identified through geological methodologies. Further, in Italy, due to the prevailing construction typologies, magnitude 5.5 is usually seen as the lower limit for which a crustal earthquake can cause such shaking as to create significant damage to buildings.

The main DISS elements are: (i) the individual seismogenic source: a simplified and 3D representation of the fault plane; (ii) the composite seismogenic source: an elongated region characterized by a set of aligned seismogenic sources; (iii) the debated seismogenic source: an active fault proposed in the literature as a potential seismogenic source but was not considered certain enough; (iv) the subduction zone: a complex 3D representation of the detachment at the base of the accretionary prism. Each record is supported by information, commentary, and references (fig. 2.12).

The individual seismogenic sources can be used for scenario studies, while the composite ones are used, together with the seismicity catalogues, to develop probabilistic models of seismic hazard. For further information on the DISS, you can watch the video at https://www.youtube.com/watch?v=4ptmcpKUvRM.

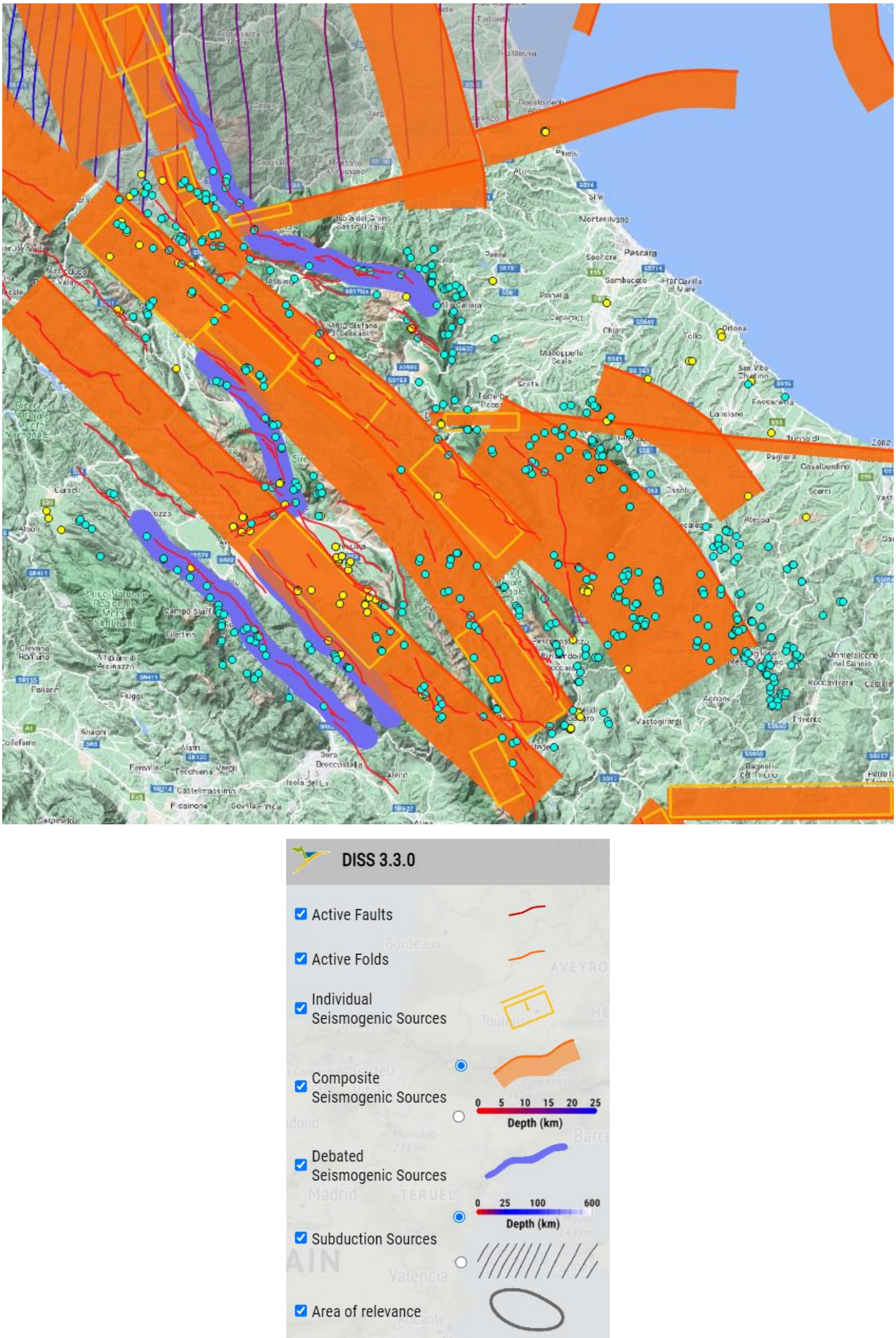

Figure 1.11: View for the Abruzzi region of the DISS version 3.3.0 by INGV (DISS Working Group, 2021) with the potential monitoring sites (spring: blue dot, well: yellow dot)

Figure 2.12: DISS version 3.3.0 by INGV (DISS Working Group, 2021): example of information, commentary, and references referred to the seismogenic source.

2.2.2 Seismic macrozonation

The “Seismic macrozonation” folder contains the informational levels shown in figure 2.1. This group includes the seismogenic zonation ZS9 by INGV (https://data.ingv.it/dataset/344#additional-metadata) (Meletti and Valensise, 2004). It is stored in the QGIS project as WMS found on the Italian Geoportal of the Ministry of the Environment (link http://www.pcn.minambiente.it/) and the georeferenced “Map of the seismogenic zones and seismotectonic provinces” by Lavecchia et al. (2006).

The seismogenic zonation ZS9 by INGV is a seismic source model for Italy to be used as an input for probabilistic seismic hazard assessment (https://data.ingv.it/dataset/344#additional-metadata) (Meletti et al., 2004; Meletti and Valensise, 2004). ZS9 has been elaborated based mainly on the information of the DISS 2.0 (Database of Individual Seismogenic Source) catalog (Valensise et al., 2001). The main informative data reported in the QGIS project are the limits, the effective depth, the dominant fault mechanism, and the soft boundaries of the identified seismogenic zones (figs. 2.13-2.15). ZS9 is made up for the Italian territory of more than 30 zones where earthquakes with Mw ≥ 5 can occur.

Within the Abruzzi region, from NE toward SW, the zones 917, 918, 923 and 920 fall. They are NW-SE elongated like the Apennine chain (fig. 2.13). The zone 923 is located within the axial zone of Apennines, which include faults and fault systems linked to the NE-SW directed Apennine extensional area. In the zone 923, the seismogenic sources, responsible for the earthquakes with the highest magnitude that hit the central Apennines, fall. The zone 923 can be considered the zone with the highest seismic hazard of the Abruzzi region. The zone 920 represents the transition toward SW to the peri-Tyrrhenian extensional areas. It is characterized by low-energy seismicity that only occasionally reaches high magnitude values. Instead, zone 918 falls within a transition strip with mixed characteristics, where different mechanisms coexist (essentially compressive regime to the NW and extensional regime to the SE). Finally, zone 2017 represents a full compressive area dominated by buried thrust faults (expected failure mechanisms: thrust and strike-slip).

The boundaries between the zones shown in the "Limits of seismogenic zones" are represented by using two different colors: black and blue. The black boundary defines the boundaries that are exclusively derived from tectonic or geologic-structural information. The blue boundary defines subdivisions of zones with the same deformation style but with different seismic characteristics, such as spatial distribution and frequency of the events, maximum expected magnitude, etc. These two differences are significant for a correct assessment of the seismic hazard (fig. 2.13).

In the “Dominant fault mechanism” layer is included all information concerning the prevalent fault mechanism for each seismogenic zone. The prevalent fault mechanism refers to the one that has the highest probability of characterizing future significant earthquakes. This mechanism has been expressed according to three types: normal fault (light blue color), reverse fault-thrust (red color), strike-slip fault (green color) and undefined mechanism (white color) (fig. 2.14).

The “Effective depth” layer contains information about the seismogenic layers and their corresponding effective depth for each seismogenic zone. The “effective depth” is the depth to which the maximum number of earthquakes occur. In this informative layer, yellow, green, blue, and red colors respectively represent an effective depth of about 3 -5 km, 6 – 7 km, 8 – 12 km, 13 – 20 Km (fig. 2.15).

Considering the above-mentioned seismotectonic setting of the Abruzzi region, the most interesting area where to locate the potential radon monitoring sites should be the zone 923 characterised by NW-SE directed normal faults, normal faulting earthquakes and hypocenter depths about 13-20 km (figs. 2.16-2.18).

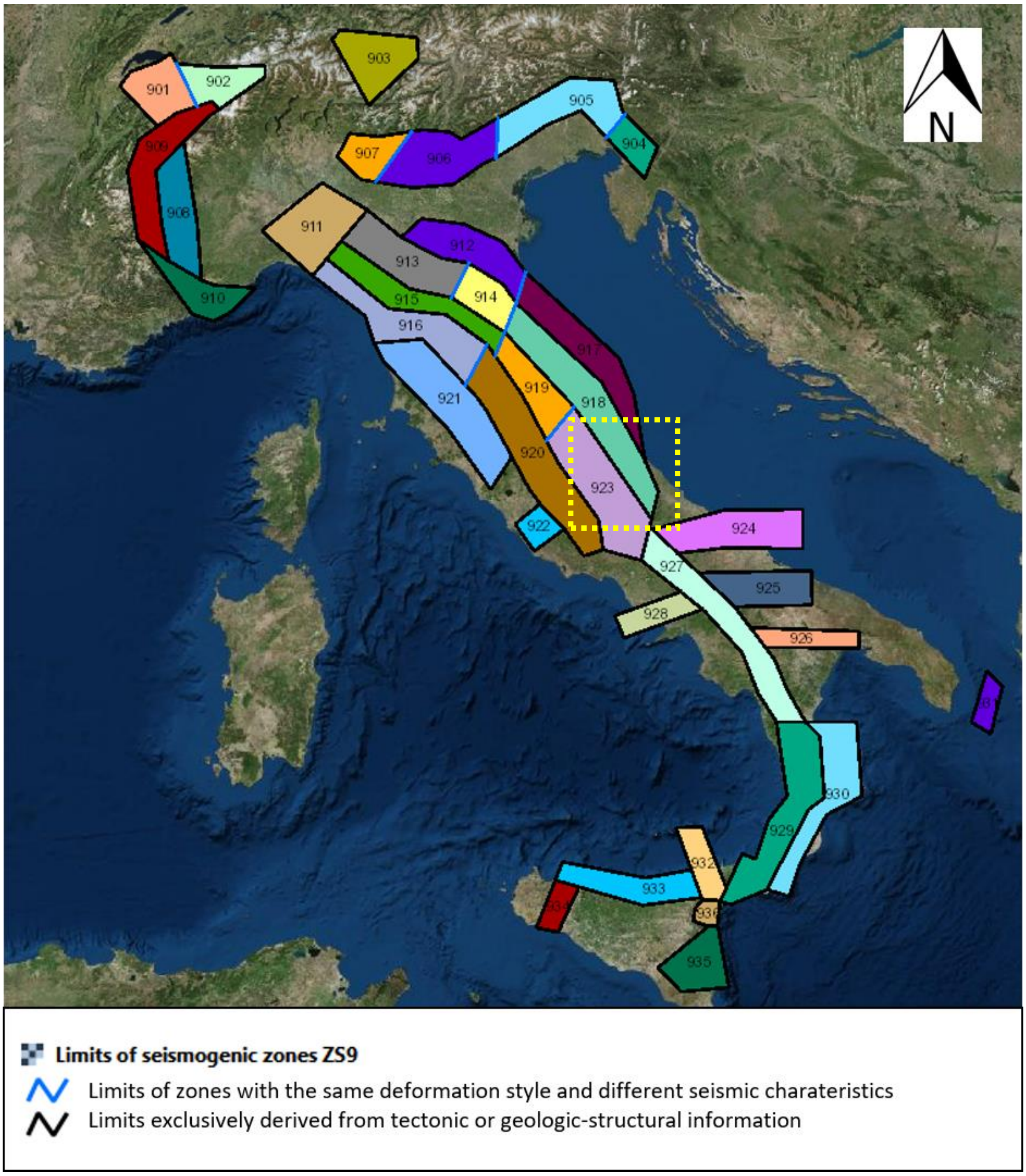

Figure 2.13: The seismogenic zones for the Italian territory of the zonation ZS9: "Limits of seismogenic zones". Square: Abruzzi region

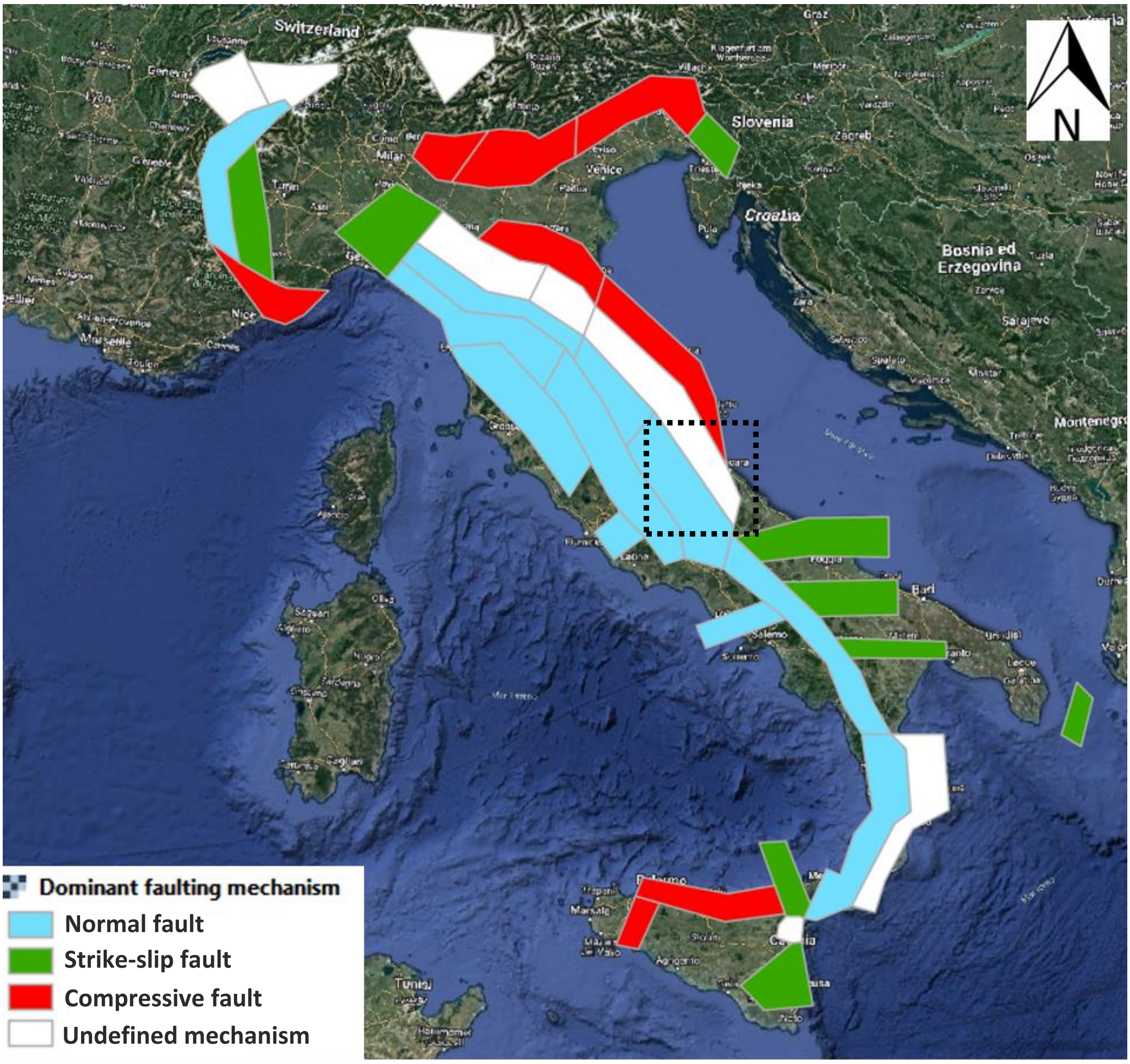

Figure 2.14 The seismogenic zones for the Italian territory of the zonation ZS9: "Dominant fault mechanism". Square: Abruzzi region

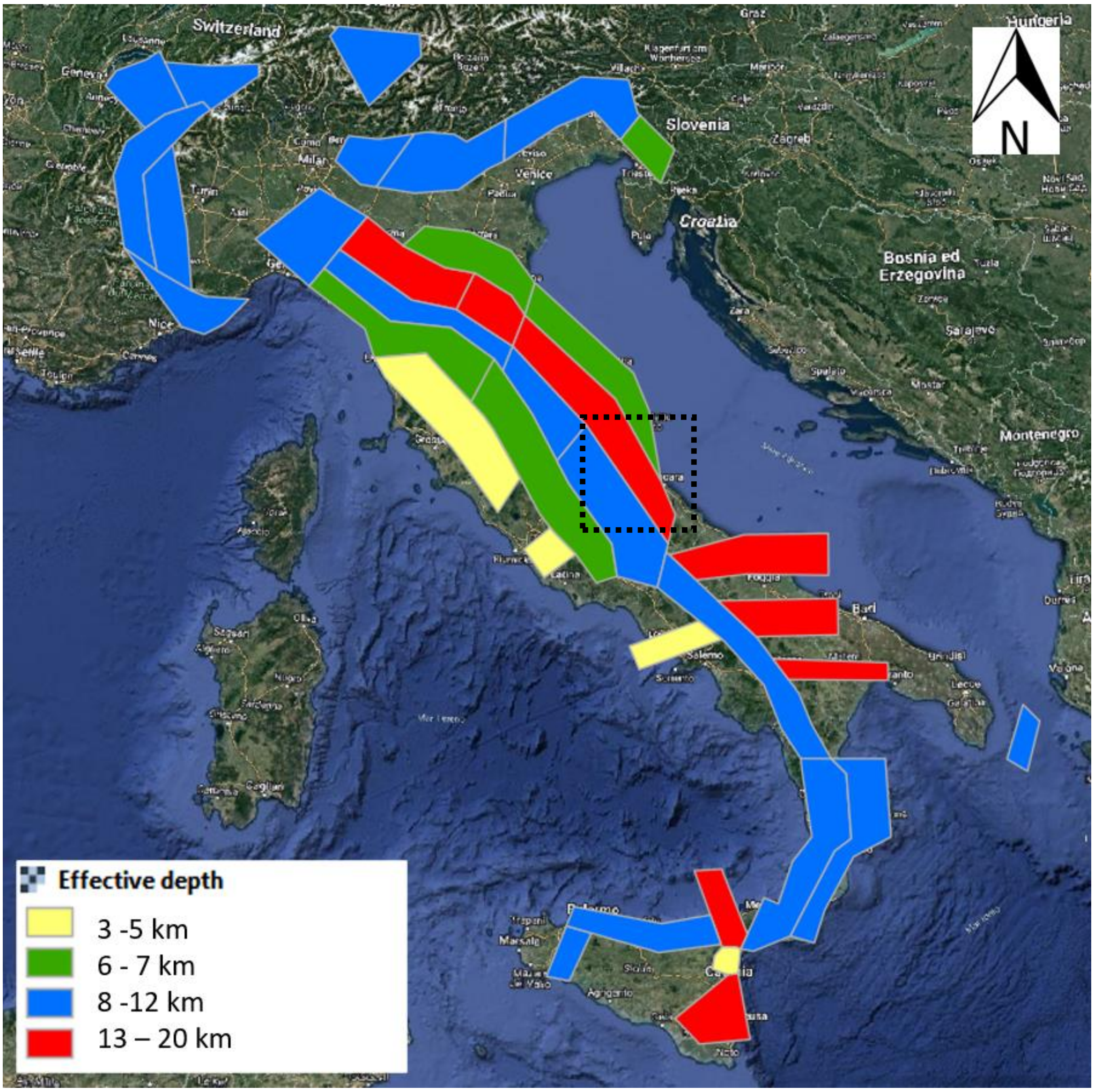

Figure 2.15: The seismogenic zones for the Italian territory of the zonation ZS9: "Effective depth ". Square: Abruzzi region

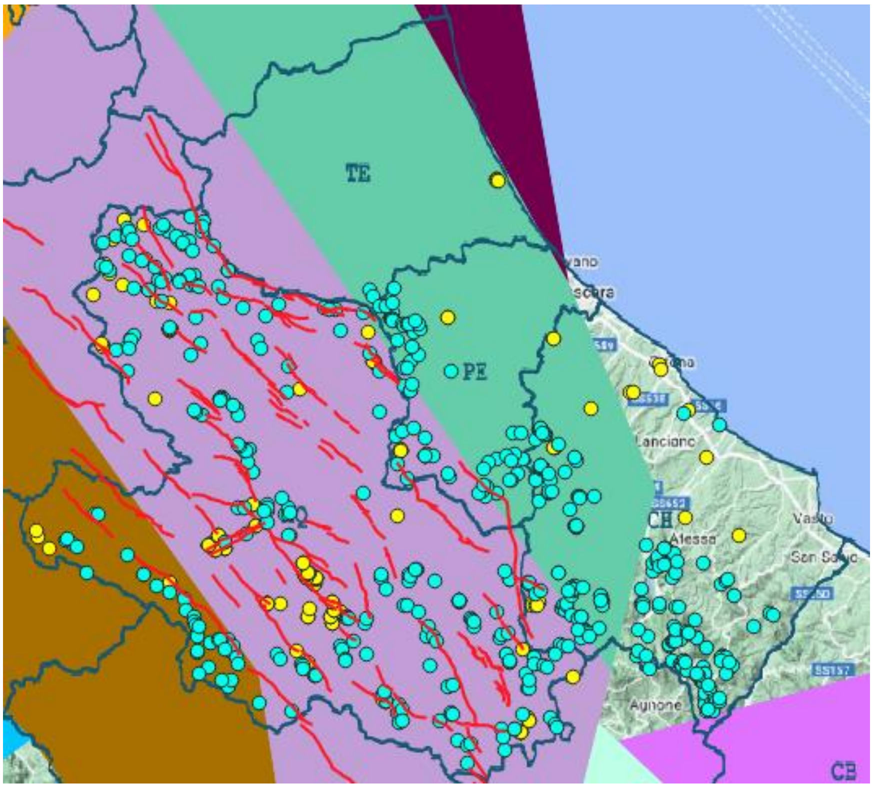

Figure 2.16: Seismogenic zones ZS9 by Meletti et al. (2004), active faults by Carafa et al. (2022) and potential monitoring sites (spring: blue dot, well: yellow dot). From SW toward NE: zone 918: brown, zone 923: Violet, zone 918: green, zone 917: dark brown

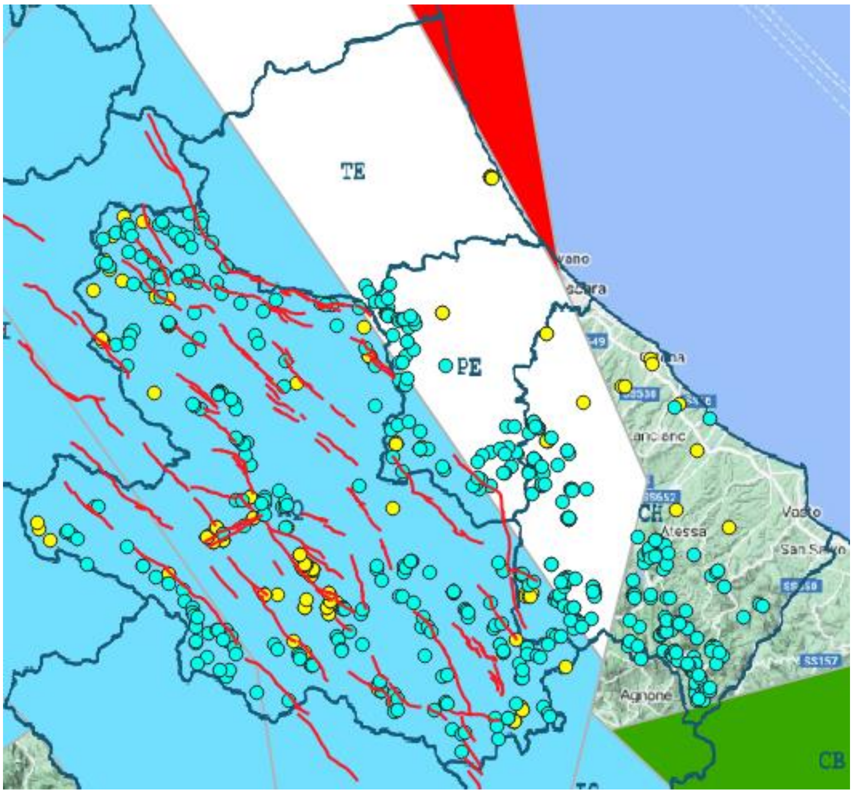

Figure 2.17: “Dominant fault mechanisms” of earthquakes from Seismogenic zones ZS9 by Meletti et al. (2004), active faults by Carafa et al. (2022) and potential monitoring sites (spring: blue dot, well: yellow dot). Earthquake rupture mechanism: compressive fault-thrust: red, mixed faulting: compressive and normal faults: white, normal faulting: light blue

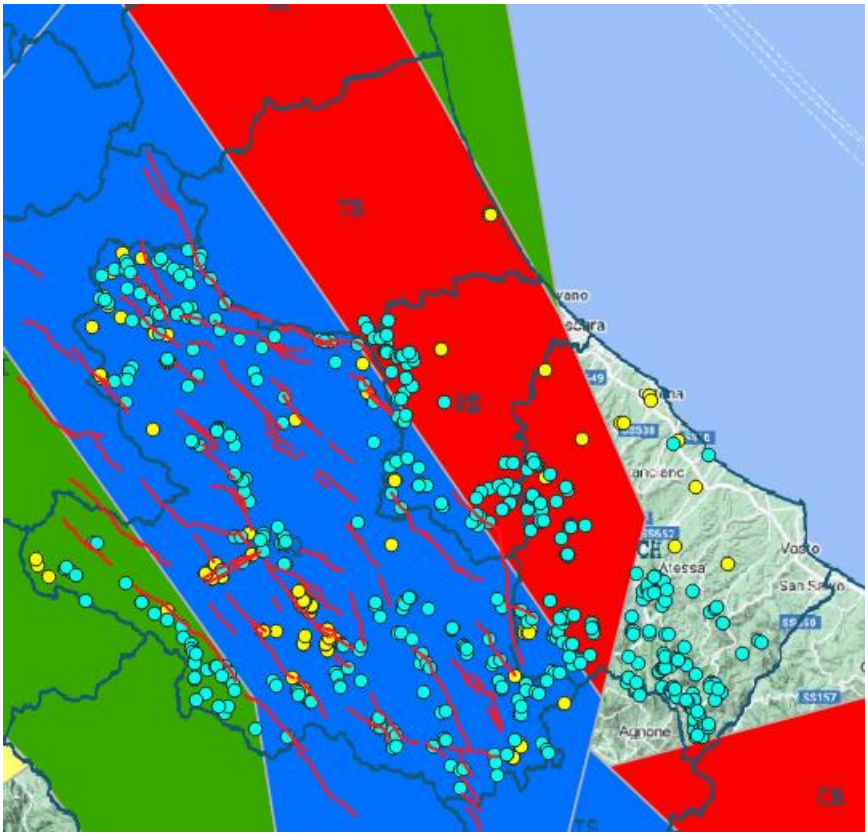

Figure 2.18: “Effective depth” of earthquakes from Seismogenic zones ZS9 by Meletti et al. (2004), active faults by Carafa et al. (2022) and potential monitoring sites (spring: blue dot, well: yellow dot). Hypocentral depth: 6-7 km: green, 8-12 km: red, 13-20 km: blue

2.2.3 Active faults

The “FAC ITHACA” folder contains information about the active and capable faults that affect the Italian territory, cataloged by the Geological Survey of Italy (ISPRA) (http://sgi.isprambiente.it/ithaca/viewer/index.html).

The ITHACA project, which stands for ITaly HAzard from CApable faults, is a fundamental tool for: a) environmental and seismic hazard analysis, b) territorial planning, and c) Civil Protection emergency management. The active and capable faults are here classified based on their latest activation and kinematics (fig. 2.19).

Further, the INGV database of active faults by Carafa et al. (2022) ("Carafa&al_2022_faultDatabase") has been added in the QGIS project. For the detailed description of these active faults see the deliverable D2.1.

In figure 2.20, by way of example, the attribute table of the database by Carafa et al. (2022) is reported. The attribute table is composed of 7 columns:

1. OBJECTID is a progressive number assigned to the active fault;
2. Code refers to the fault code;
3. Name irefers to the tectonic structure’s name;
4. Dip_dir refers to the fault dip direction;
5. Outcrop refers to the field characteristics of the faults: certain, buried and inferred;
6. Throw_rate in mm/year;
7. 95_IC refers to the the 95% confidence interval with respect to the median of the throw rate distribution.

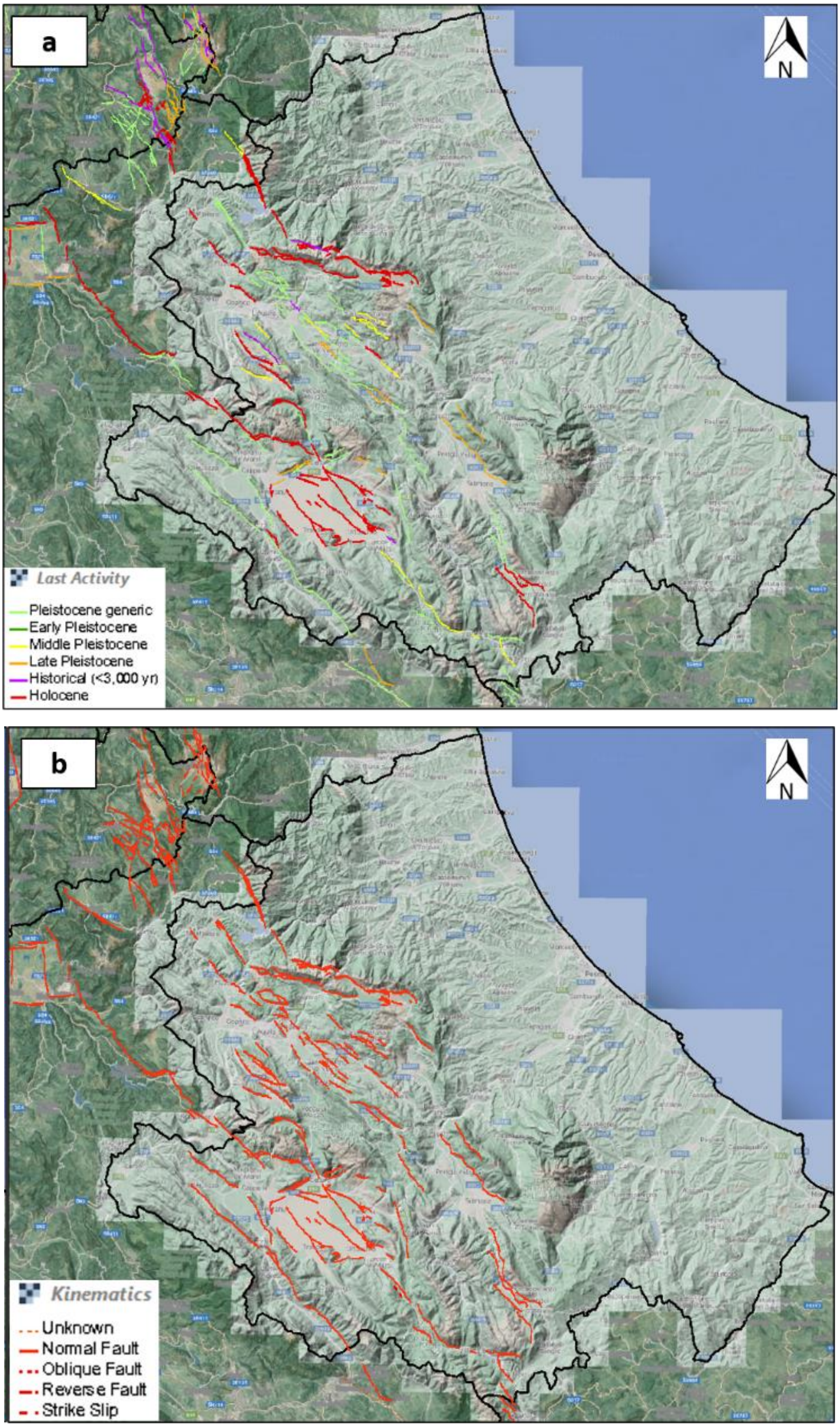

Figure 2.19: Zoom-in of the ITHACA catalog for the Abruzzi region (black contour line) in which the active faults are classified based on the last activity (a) and fault kinematics (b)

	OBJECTID	code	name	dip_dir	outcrop	throw_rate	95_IC
85	113	F0046N	Campo Imperatore 2	SSW	inferred	0.8	0.65-0.94
86	116	F0047N	Campo Imperatore 3	SSW	buried	0.26	0.13-0.40
87	118	F0047N	Campo Imperatore 3	SSW	certain	0.26	0.13-0.40
88	119	F0046N	Campo Imperatore 2	SSW	certain	0.8	0.65-0.94
89	120	F0046N	Campo Imperatore 2	SSW	certain	0.8	0.65-0.94
90	122	F0046N	Campo Imperatore 2	SSW	inferred	0.8	0.65-0.94
91	125	F0047N	Campo Imperatore 3	SSW	certain	0.26	0.13-0.40
92	126	F0046N	Campo Imperatore 2	SSW	buried	0.8	0.65-0.94
93	127	F0046N	Campo Imperatore 2	SSW	buried	0.8	0.65-0.94
94	128	F0046N	Campo Imperatore 2	SSW	certain	0.8	0.65-0.94
95	129	F0046N	Campo Imperatore 2	SSW	certain	0.8	0.65-0.94
96	130	F0048N	Assergi 1	SSW	certain	0.21	0.03-0.55
97	131	F0050N	Montecristo 1	SW	certain	0.32	0.07-0.69
98	132	F0051N	Montecristo 2	SW	certain	0.26	0.04-0.61
99	133	F0052N	Mt. San Franco	SSW	certain	0.84	0.50-1.47
100	134	F0044N	Carsoli	SW	certain	0.36	0.26-0.49
101	135	F0044N	Carsoli	SW	inferred	0.36	0.26-0.49
102	136	F0044N	Carsoli	SW	certain	0.36	0.26-0.49
103	137	F0044N	Carsoli	SW	certain	0.36	0.26-0.49
104	138	F0044N	Carsoli	SW	certain	0.36	0.26-0.49
105	142	F0065N	Cassino	SW	certain	0	NULL
106	145	F0001N	Cassino	SW	certain	0.32	0.17-0.50
107	147	F0065N	Cassino	SW	inferred	0	NULL

Figure 2.20: Attribute table active faults database of the Abruzzi region by Carafa et al. (2022)

The database of Carafa et al. (2022) contains also the seismogenic sources represented by the so-called seismogenic boxes (i.e. the active fault plane projection on surface) (fig. 2.21).

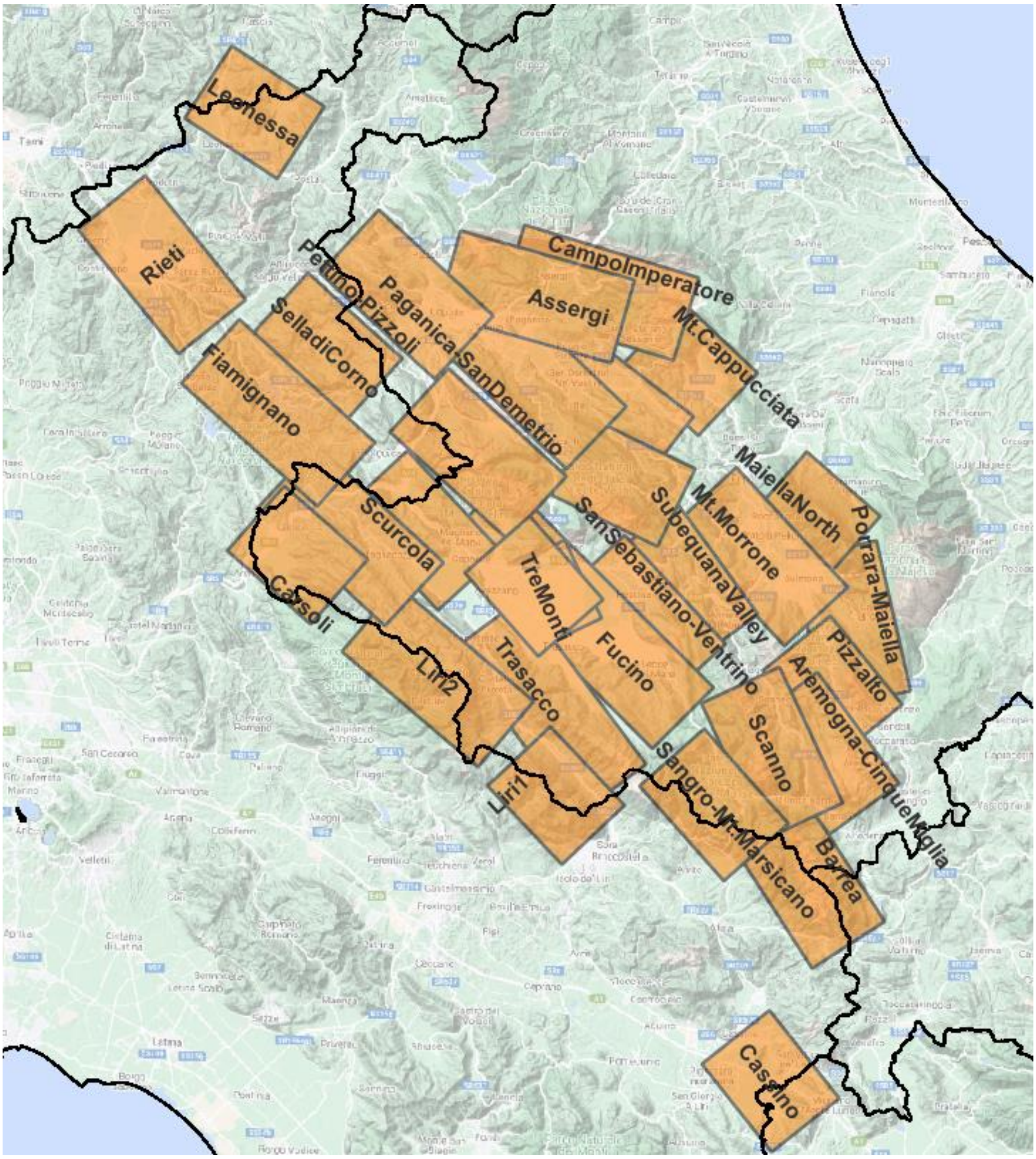

Figure 2.21: The seismogenic boxes (i.e. the active fault plane projection on surface) representative of the seismogenic sources for the Abruzzi region (Carafa et al., 2022)

2.3 References

Bigi, G., Coli, M., Cosentino, D., Parotto, M., Praturlon, A., Sartori, R., Scandone, P., Turco, E., 1992. Structural Model of Italy - Sheet 4 at 1:500,000 scale. CNR, SELCA, Firenze. [WWW Document]

https://drive.google.com/file/d/1WGFMNTJD9oZXU-3DvAmoqohq-3hLX7N3/view

(accessed 4.4.23).

Carafa, M. M. C., Di Naccio, D., Di Lorenzo, C., Kastelic, V., Bird, P., 2022. A meta-analysis of fault slip rates across the central Apennines. Journal of Geophysical Research: Solid Earth, 127, e2021JB023252. https://doi.org/10.1029/2021JB023252

DISS Working Group, 2021. Database of Individual Seismogenic Sources (DISS), version 3.3.0: A compilation of potential sources for earthquakes larger than M 5.5 in Italy and surrounding areas. Istituto Nazionale di Geofisica e Vulcanologia (INGV). https://doi.org/10.13127/diss3.3.0

Geological Survey of Italy, 2023. Mosaic of the geological maps of Italy at the scale 1:50,000 (CARG project). [WWW Document]

http://sgi2.isprambiente.it/arcgis/rest/services/raster/geo_50k_italia/ImageServer

(accessed 4.4.23)

Guidoboni, E., Ferrari, G., Mariotti, D., Comastri, A., Tarabusi, G., Sgattoni, G., Valensise, G., 2018. CFTI5Med, Catalogo dei Forti Terremoti in Italia (461 a.C.-1997) e nell'area Mediterranea (760 a.C.-1500) [Catalog of Severe Earthquakes in Italy (461 BC-1997) and in the Mediterranean area (760 BC-1500)]. Istituto Nazionale di Geofisica e Vulcanologia (INGV). https://doi.org/10.6092/ingv.it-cfti5

Lavecchia, G., Boncio, P., Brozzetti, F., De Nardis, R., Pace, B., Visini, F., 2006. Studio della Pericolosità sismica della Regione Abruzzo. Internal report "Studio della Pericolosità sismica della Regione Abruzzo e ulteriori attività di supporto tecnico-scientifico da realizzare nell'ambito del Coordinamento delle Università abruzzesi per la ricerca applicata alla mitigazione del Rischio sismico" [Study of the seismic hazard of the Abruzzo Region and technical-scientific support activities to be carried out in the context of the Coordination of the Abruzzi Universities for research applied to the mitigation of seismic risk]. Agreement between Abruzzi region and GeoSisLab – Dipartimento di Scienze della Terra, Università di Chieti, pp. 31. chrome-extension://efaidnbmnnnibpcajpcglclefindmkaj/https://eppursimuoveaq.files.wordpress.com/2011/03/pericolositc3a0-sismica-abruzzo_lavecchia-etal2006.pdf

Meletti, C., Galadini, F., Valensise, G., Stucchi, M., Basili, R., Barba, S., Vannucci, G., Boschi, E., 2004. Zonazione sismogenetica ZS9 [Data set]. Istituto Nazionale di Geofisica e Vulcanologia (INGV). https://doi.org/10.13127/sh/zs9

Meletti, C., Valensise, G., 2004. Zonazione sismogenetica ZS9 – App.2 al Rapporto Conclusivo [ZS9 seismogenic zoning – Appendix 2 to the Final Report]. In: Working Group MPS (2004). Drafting of the Seismic Hazard map required by the Italian Ordinance PCM 3274 of March, 20 2003. Conclusive report for the Italian Civil Protection Department, INGV, Milan-Rome, pp. 65

Valensise, G., Pantosti, D., Basili, R., Bordoni, P., Burrato, P., Nappi, R., Spinelli, A., 2001. Database of potential sources for earthquakes larger than M 5.5 in Italy (DISS version 2.0). Annals of Geophysics, vol. 44, Suppl. 1, with CD-ROM. Available from: https://www.annalsofgeophysics.eu/index.php/annals/article/view/3562

Vezzani, L., Ghisetti, F., 1998. Carta geologica dell'Abruzzo [Geological map of Abruzzi], at 1: 100000 scale. SELCA, Firenze.

3 GIS map and database of geology and seismotectonics of the central Ionian Islands & Corinth Gulf

In this section the workflow and the structure of the developed GIS databases and the corresponding maps about the geology and the seismotectonic setting of central Ionian Islands and Gulf of Corinth, Greece, is presented. It includes details about the data compiled for the developed databases (geological formations and active faults of the selected areas), along with the descriptions concerning the structure of the related databases. Examples of geological and seismotectonic maps for both the central Ionian Islands and Gulf of Corinth using the associated shapefiles, are also given.

3.1 Geology GIS database and maps of central Ionian Islands and Corinth Gulf

For the development of the GIS database and the associated maps concerning the geology of central Ionian Islands (Kefalonia and Lefkada) and Gulf of Corinth the geological formations data of each area are compiled and extracted from the available digitized geological map sheets and presented as polygons in the respective shapefiles of the database. Additionally, already published geological maps are georeferenced and stored in the database via the QGIS software. The maps are prepared by using the Digital Elevation Model (DEM) of Greece provided by the Copernicus Land Monitoring Service (https://land.copernicus.eu/imagery-in-situ/eu-dem; last accessed on April 2023) for the construction of the geomorphological base maps of selected areas.

3.1.1 Geology GIS database and maps of central Ionian Islands

The development of geological GIS database and the corresponding geological map of central Ionian Islands is implemented by accessing the geological map sheets of Bornovas (1964), Rondoyanni et al. (2007) and the Institute of Geology and Mineral Exploration (IGME). Additionally, the geological maps of Papathanasiou et al. (2021) and Lekkas and Mavroulis (2015) for Lefkada and Kefalonia Islands, respectively, are geoferererenced and also included in the developed geological GIS database.

In detail, the geological database of Lefkada Island is composed by the detailed geological formations shapefile (Lefkada_Geological_Units.shp) of the geological map sheets of Bornovas (1964) and Rondoyanni et al. (2007) as compiled by Papathanasiou et al. (2021). It is also including the simplified geoferererenced geological map provided by the latter authors. An example of elaboration of the geological data included in the database in constructing a simplified geological map for Lefkada Island is shown in Figure 3.1. Specifically, Figure 3.1 shown the geological formation extended in Lefkada Island as they grouped considering lithological and chronological criteria, using as input file the geological formations shapefile, which includes the geological information compiled from the aforementioned studies. As it is derived from the geological map of Figure 3.1, Lefkada Island is mainly composed by geological formations of the Paxos (brown and blue colors for the Flysch and marine carbonates geological units, respectively) and Ionian (dark grey and green colors for the Flysch and marine carbonates geological units, respectively) Pre-Apulian zones of the External Hellenides, along with Quaternary-Holocene coastal and Miocene marine sediments denoted with the light grey and yellow colors, respectively.

Similarly, the geology of Kefalonia Island is also composed by the geological formations of the Paxos and Ionian zones of the External Hellenides, along with both coastal and marine sediments. The spatial extend of the geological formations of Kefalonia Island, which is included in the current developed database is taken by georeferencing the detailed neotectonic map provided by Lekkas and Mavroulis (2005). Figure 3.2 shown a snapshot of the QGIS software workspace, in which the GIS database of central Ionian Islands and the georeferenced neotectonic map of Kefalonia Island is stored.

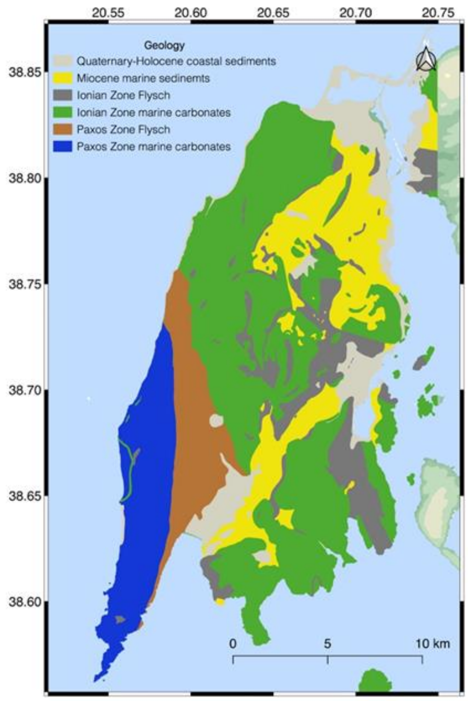

Figure 3.1: Simplified geological map of Lefkada Island, in which the geological formations are denoted with different colors according to the inset legend, using as input data the geological map sheets of Bornovas (1964) and Rondoyanni et al. (2007) as compiled by Papathanasiou et al. (2021)

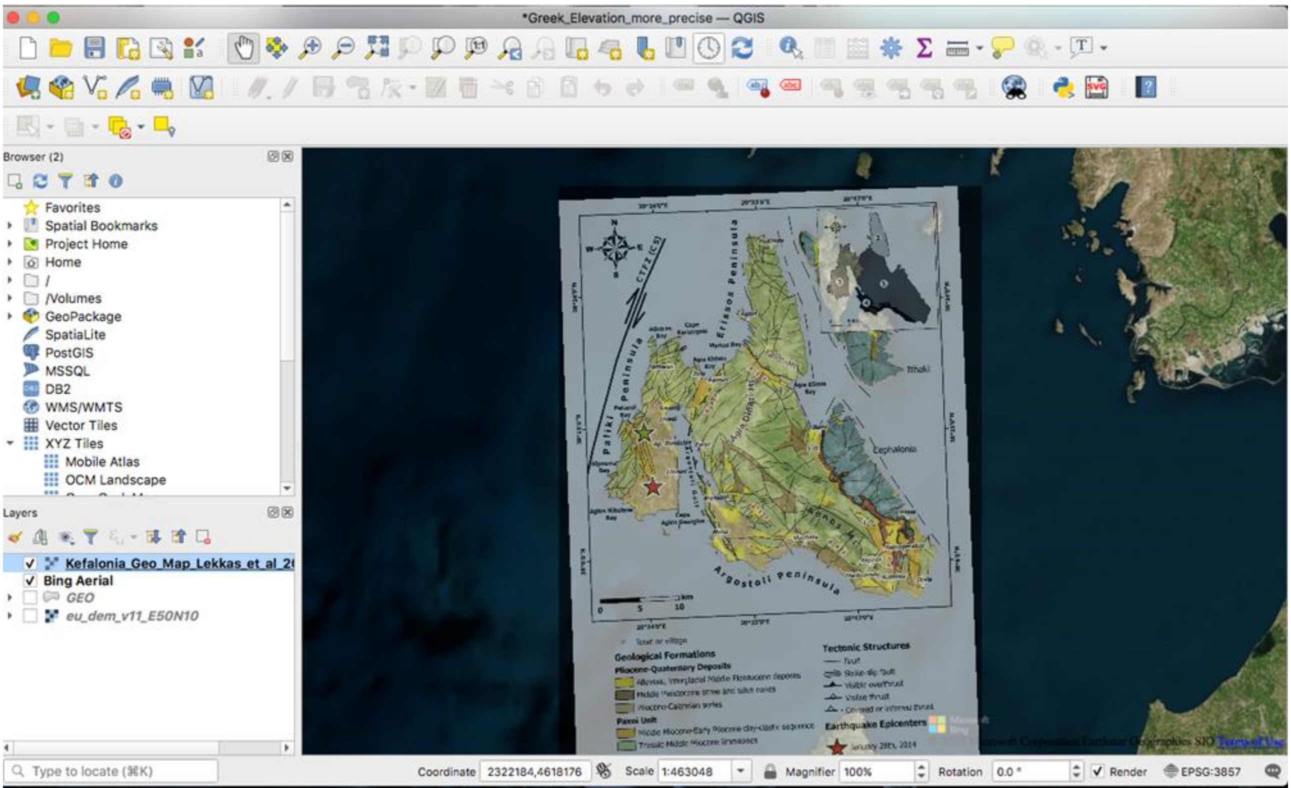

Figure 3.2: Snapshot of the QGIS Database workspace showning the georeferenced geological map of Kefalonia Island taken from Lekkas and Mavroulis (2015), which is stored in the Geological GIS Database

3.1.2 Geology GIS database and maps of Corinth Gulf

The GIS database and map of the second selected area, the Gulf of Corinth, are developed by the use the detailed geological map of Valkaniotis (2009) and the geological map sheets of the Institute of Geology and Mineral Exploration (IGME). Gulf of Corinth is composed by formations belonging to Pelagonian, Parnassos, Pindos and Gavrovo – Tripolitsa zones from its Easternmost to its Southernmost margins. Formations of the aforementioned geological zones are given in terms of discrete polygons in the detailed geological formations shapefile (Corinth_Geological_Units.shp), which is stored in the GIS Database. Figure 3.3 shown a snapshot of QGIS Database workspace, in which the geological formations shapefile (Corinth_Geological_Units.shp) is loaded.

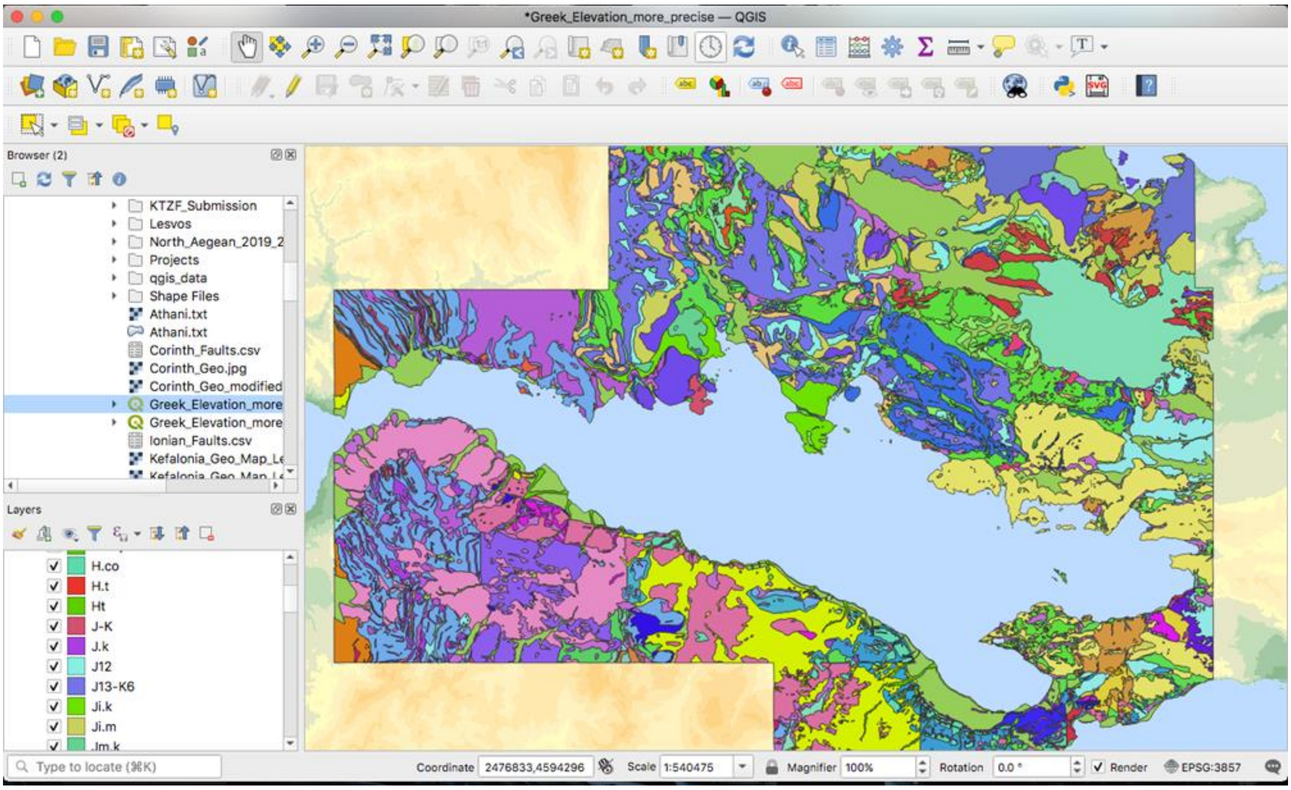

Figure 3.3: Snapshot of the QGIS Database workspace showing the loaded detailed geological formations layer of the Gulf of Corinth as compiled by Valkaniotis et al. (2009) and the geological map sheets of the Institute of Geology and Mineral Exploration (IGME). Each color represents different geological formations according to their lithology

3.2 Seismotectonic GIS database and maps of central Ionian Islands and Corinth Gulf

In this section the main characteristics and the structure of the GIS databases concerning the seismotectonics of central Ionian Islands and Gulf of Corinth are described, along with the workflow of the compilation of the including fault segments data and parameters. The maps of the main active seismic faults of both the selected areas are also presented.

The development of the databases is based upon the compilation of available seismological and geological field survey data provided by published studies, combined with information of additional fault databases. The current approach is implemented by assuming the standard source characterizations of independent ruptured segments with fixed endpoints (Schwartz, 2018). Each of the two databases consists of discrete fault segments, which defined by their structural and geometric parameters (e.g., faulting type, fault traces, fault dimensions). They are composed by the following parameters for each fault:

- the geographical coordinates of the fault segment trace.
- an identification number (Fault ID).
- the fault segment name.
- the type of faulting (normal, thrust, strike-slip).
- the geometrical and kinematic fault segment parameters (strike, dip, rake, length and width).
- the corresponding references used for the fault segment definition.

The aforementioned parameters and information are used for the construction of the source files of the two databases in .csv format (Ionian_Faults.csv and Corinth_Faults.csv). An example of the structure of source files is shown in Figures 3.4 for the case of the central Ionian Islands database. These source files are the core inputs for the development of the associated shapefiles of the databases. The resulted shapefiles include the defined fault parameters in their Attribute Tables.

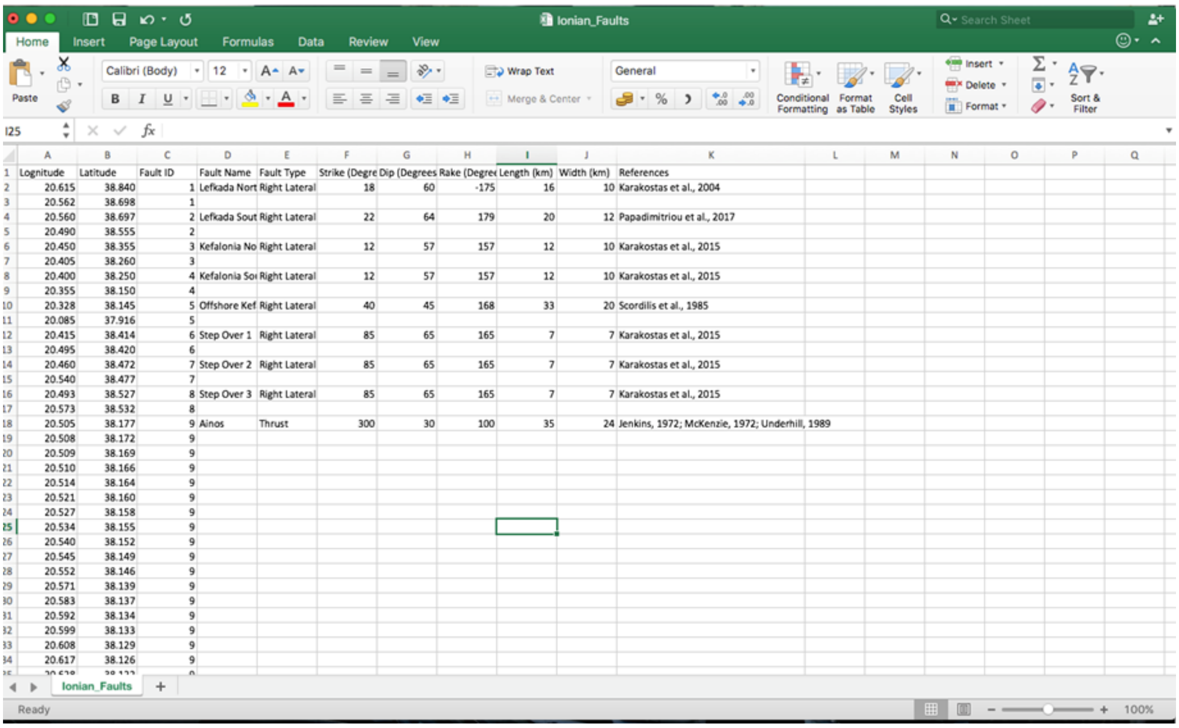

	A	B	C	D	E	F	G	H	I	J	K
1	Lognitude	Latitude	Fault ID	Fault Name	Fault Type	Strike (Degre	Dip (Degrees	Rake (Degre	Length (km)	Width (km)	References
2	20.615	38.840	1	Lefkada Nort	Right Lateral	18	60	-175	16	10	Karakostas et al., 2004
3	20.562	38.698	1								
4	20.560	38.697	2	Lefkada Sout	Right Lateral	22	64	179	20	12	Papadimitriou et al., 2017
5	20.490	38.555	2								
6	20.450	38.355	3	Kefalonia No	Right Lateral	12	57	157	12	10	Karakostas et al., 2015
7	20.405	38.260	3								
8	20.400	38.250	4	Kefalonia So	Right Lateral	12	57	157	12	10	Karakostas et al., 2015
9	20.355	38.150	4								
10	20.328	38.145	5	Offshore Kef	Right Lateral	40	45	168	33	20	Scordilis et al., 1985
11	20.085	37.916	5								
12	20.415	38.414	6	Step Over 1	Right Lateral	85	65	165	7	7	Karakostas et al., 2015
13	20.495	38.420	6								
14	20.460	38.472	7	Step Over 2	Right Lateral	85	65	165	7	7	Karakostas et al., 2015
15	20.540	38.477	7								
16	20.493	38.527	8	Step Over 3	Right Lateral	85	65	165	7	7	Karakostas et al., 2015
17	20.573	38.532	8								
18	20.505	38.177	9	Ainos	Thrust	300	30	100	35	24	Jenkins, 1972; McKenzie, 1972; Underhill, 1989
19	20.508	38.172	9								
20	20.509	38.169	9								
21	20.510	38.166	9								
22	20.514	38.164	9								
23	20.521	38.160	9								
24	20.527	38.158	9								
25	20.534	38.155	9								
26	20.540	38.152	9								
27	20.545	38.149	9								
28	20.552	38.146	9								
29	20.571	38.139	9								
30	20.583	38.137	9								
31	20.592	38.134	9								
32	20.599	38.133	9								
33	20.608	38.129	9								
34	20.617	38.126	9								

Figure 3.4: The structure of the source file of the seismotectonic database of central Ionian Islands, composed by the coordinates of fault segment trace, the fault ID, the fault segment name and type, the geometrical and kinematic parameters of fault segment (strike, dip, rake) in degrees, fault segment dimensions (length, width) in km and the corresponding references

Figure 3.5 shown an example of the development of the seismotectonic map of Gulf of Corinth with the use of QGIS software. Specifically, in the left part of Figure 3.4 the uploaded base map and the shapefile of active faults of Gulf of Corinth (Corinth_2.shp; 2nd version of the Gulf of Corinth Fault Database), whereas in the middle part of Figure 3.5 the projections of the active faults included in the Database on the geomorphological base map are shown with the solid red lines. The thick solid line represents the selected fault segment of which the associated parameters are included in the Attribute Table of the corresponding shapefile in the right part of Figure 3.5.

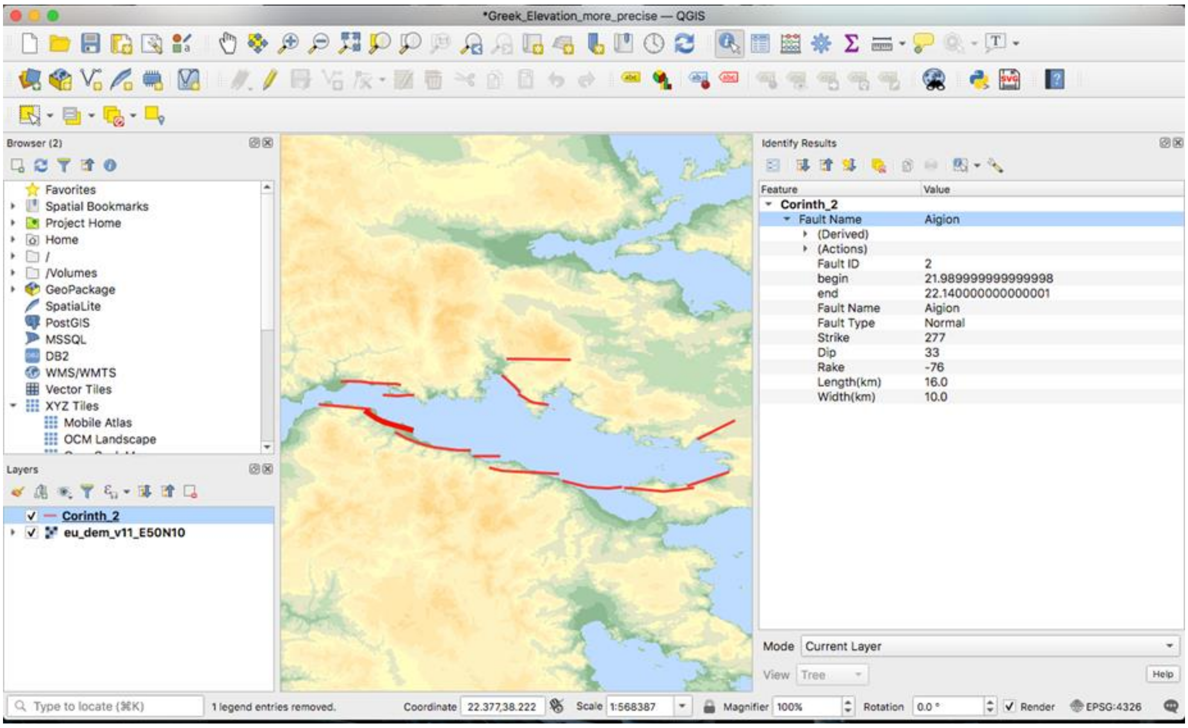

Figure 3.5: Example of the preparation of the seismotectonic map of Gulf of Corinth using the corresponding database of active faults (Corinth_Faults.csv) via the QGIS software. The uploaded base map and the shapefile of active faults of Gulf of Corinth (Corinth_2.shp) are shown in the left part, whereas the projections of the active faults are shown in the middle one (solid red lines). Thick solid red line depicts the selected fault segment (Aigion; Fault ID: 2) of which the associated parameters are included in the Attribute Table and are shown in the right part

3.2.1 Seismotectonic GIS database and maps of central Ionian Islands

The main seismotectonic feature of central Ionian Islands is the Kefalonia Transform Fault Zone (KTFZ), which is characterized by right-lateral strike slip motion with significant thrust component (Scordilis et al., 1985; Kiratzi and Langston, 1991; Papadimitriou, 1993; Louvari et al., 1999) and can be distinguished into two main branches, namely the Lefkada branch covering its northern part, striking NNE-SSW and the Kefalonia branch to the south with a slightly different NE-SW strike.

The database of active fault segments extended within central Ionian Islands is composed by the 5 main right-lateral fault segments, which are associated with large earthquakes (M_w≥6.0) occurred during the instrumental period of seismicity (since 1983) and allowing their detailed definition. For this definition the studies of Scordilis et al. (1985), Karakostas et al. (2004), Karakostas et al. (2015) and Papadimitriou et al. (2017) are used. Additionally, Karakostas et al. (2015) proposed the existence of a transition zone of 3 secondary parallel step-over fault segment between Kefalonia and Lefkada Islands, which are also included in the current database. The secondary Athani-Dragano strike-slip fault, which is sub-parallel to the Lefkada branch fault segments of KTZF (Rondoyanni et al., 2012), is included in the Database, as well.

The southeastern part of Kefalonia Island is also characterized by the existence of thrust faulting, as geological mapping evidences. The main active thrust faults are the Mount Ainos fault segment and the Argostoli ones. For the definition of the structural and geometrical parameters of those faults the available data from the studies of Jenkins (1972), McKenzie (1972) and Underhill (1989) are combined.

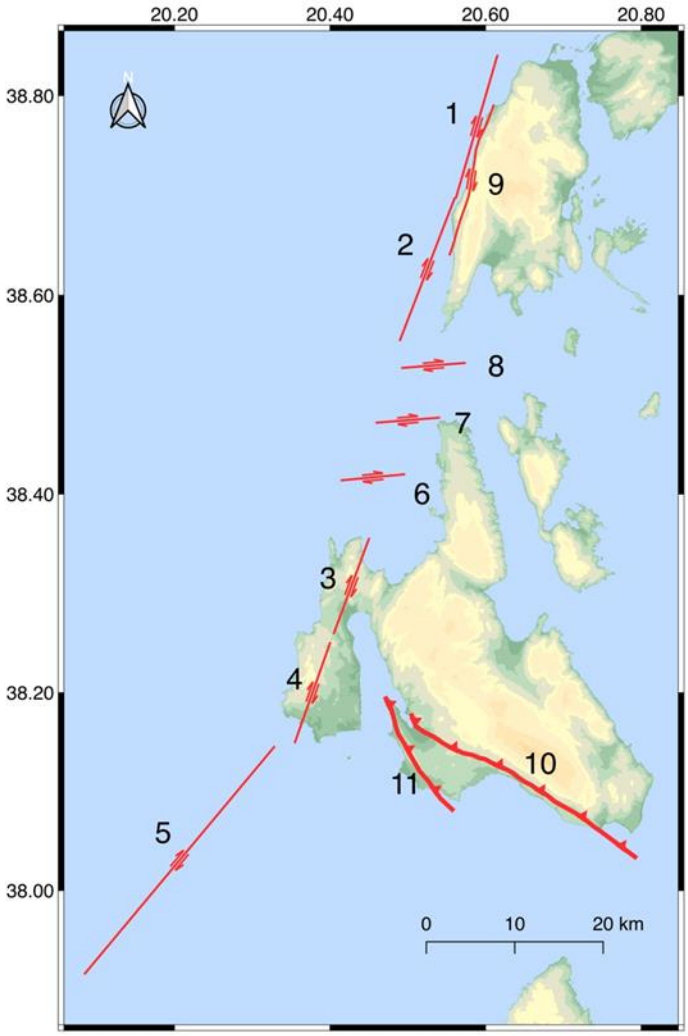

Figure 3.6: Geomorphological map of central Ionian Island, along with the 10 active fault segments of the related seismotectonic database. Fault segments are depicted as solid red lines with different symbol styling in accordance with its faulting type, along with their Fault ID (1: North Lefkada fault segment; 2: South Lefkada fault segment; 3: North Kefalonia fault segment; 4: South Kefalonia fault segment; 5: offshore Kefalonia fault segment; 6-8: Step Over fault segments; 9: Athani-Dragano fault segment; 10: Ainos fault segment; 11: Argostoli fault segment)

The final seismotectonic database of central Ionian Island (in both .csv and .shp file formats) consists of 11 active fault segments (the 5 main right-lateral fault segments of KTFZ, the 3 secondary step-over fault segments, along with Athani-Dragano one, and the 2 thrust fault segments), whose parameters are compiled from the aforementioned studies). Figure 3.6 shown the resulted map, in which the fault segments traces are projected on the geomorphological base map. Its fault segment is depicted as a solid red line with different symbol styling in accordance with its faulting type, along with its assigned Fault ID number.

3.2.2 Seismotectonic GIS database and maps of Corinth Gulf

The Gulf of Corinth is one of the most seismically active areas of Greece with a large number of strong (M_w≥6.0) earthquakes, both historical (such as the Heliki earthquake with M=6.8 occurred in 373 BC) and instrumental (such the sequence of strong earthquakes during 1981 in the Gulf of Alkyonides with M_w=6.7,

M_w=6.4 and M_w=6.3, occurred on February 24 and 25 and March 4, respectively). Corinth Gulf is characterized by normal faulting due to the main extensional stress field of the Aegean back-arc region.

The area of the Gulf of Corinth is one of the most studied, which has resulted in the detailed identification of its main active faults, which are distributed along its northern and southern coastlines. The database of active fault segments is created by compiling a series of already published seismological, seismotectonic and geological studies (Marinatos, 1960; Armijo et al., 1996; Hubert et al., 1996; Morewood and Roberts, 1999; Stefatos et al., 2002; Pantosti et al., 2004; Bernard et al., 2006; Valkaniotis, 2009; Console et al., 2013; Marinou et al., 2015), along with the available fault parameters and data included in two fault databases of the broader Aegean area, namely the database of active faults of Papazachos et al. (2001) and the one of the National Observatory of Athens (NOA Faults Database; Ganas, 2020).

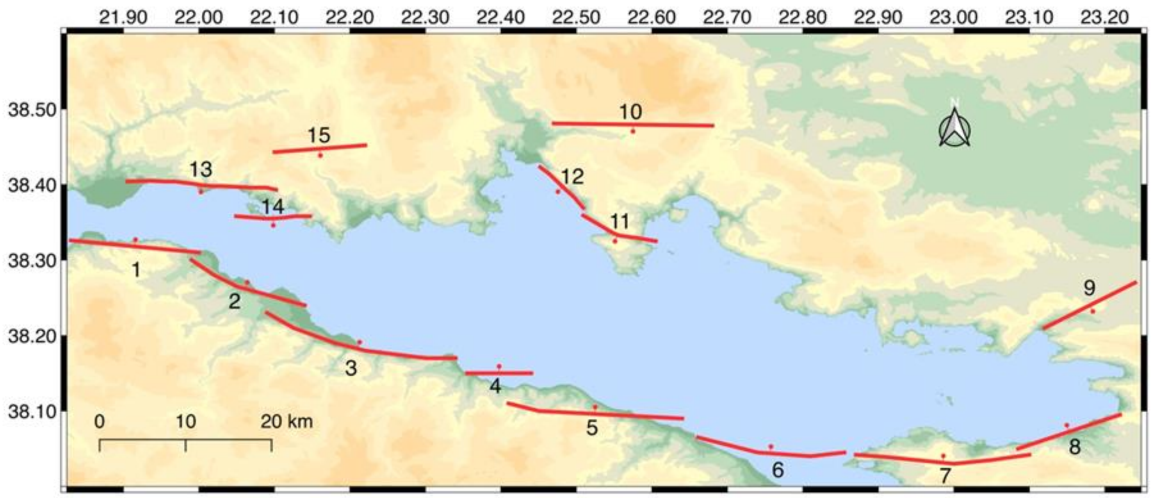

Figure 3.7: Geomorphological map of Gulf of Corinth, along with the 15 active normal fault segments of the related seismotectonic database. Fault segments are depicted as solid red lines along with their Fault ID (1: Psathopyrgos fault segment; 2: Aigion fault segment; 3: Heliki fault segment; 4: Akrata fault segment; 5: Xylokastro fault segment; 6: Perachora fault segment; 7: Schinos fault segment; 8: Alepochori fault segment; 9: Kapareli fault segment; 10: Delfoi fault segment; 11: Sykia fault segment; 12: Makrygialos fault segment; 13: Marathias fault segment; 14: Trizonia fault segment; 15: Lidoriki fault segment)

The current seismotectonic database is composed by 15 active normal faults. The 8 out of the 14 active faults are extended along the southern coastlines of Corinth Gulf, having a gradual change in their strike from 270°–280° to 260°–270° from west to east, while they are dipping to the north with angles varying between 30° and 45°. The rest of the active normal faults (7 out of the 15) are bounding both the northern (6 faults segments) and the southeastern (1 fault segment) margins of Corinth Gulf. Figure 3.6 shown the map of the projected traces of 14 active normal faults, included in developed database. Its active fault is depicted as a solid red line, along with its assigned Fault ID number.

3.3 References

Armijo, R., Meyer, B., King, G. C. P., Rigo, A., Papanastassiou, D., 1996. Quaternary evolution of the Corinth Rift and its implications for the Late Cenozoic evolution of the Aegean. Geophys. J. Int. 126, 11–53.

Bernard, P., Briole, P., Meyer, B., Lyon-Caen, H., Gomez, J.-M., Tiberi, C., Berge, C., Cattin, R., Hatzfeld, D., Lachet, C., Lebrun, B., Deschamps, A., Courboulex, F., Larroque, C., Rigo, A., Massonet, D., Papadimitriou, P., Kassaras, I., Diagourtas, D., Makropoulos, K., Veis, G., Papazisi, E., Mitsakaki, C., Karakostas, V., Papadimitriou, E., Papanastassiou, D., Chouliaras, G., Stavrakakis, G., 1997. The Ms = 6.2, June 15, 1995 Aigion earthquake (Greece): Evidence for low angle normal faulting in the Corinth rift. J. Seismol. 1, 131–150. htpps://doi.org/10.1023/A:1009795618839.

Bornovas, J., 1964. Géologie de l'île de Lefkade, Geol. Geophys.Res. 10, 14.

Console, R., Falcone, G., Karakostas, V., Murru, M., Papadimitriou, E., Rhoades, D., 2013. Renewal models and coseismic stress transfer in the Corinth Gulf, Greece, fault system. J. Geophys. Res. 118, 3655–3673. https://doi.org/10.1002/jgrb.50277.

Ganas, A., 2020. NOAFAULTS KMZ layer Version 3.0 (2020 update) (Version V3.0) [Data set]. Zenodo. doi:10.5281/zenodo.4304613.

Hubert, A., King, G., Armijo, R., Meyer, B., Papanastassiou, D., 1996. Fault re–activation, stress interaction and rupture propagation of the 1981 Corinth earthquake sequence. Earth Planet. Sci. Lett. 142, 573–585.

Jenkins, D.A.L., 1972. Structural development of western Greece. Am. Assoc. Pet. Geol. Bull. 56, 128-149.

Karakostas, V., Papadimitriou, E., Papazachos, C., 2004. Properties of the 2003 Lefkada, Ionian islands, Greece, Earthquake seismic sequence and seismicity triggering. Bull. Seismol. Soc. Am. 94(5), 1976–1981.

Karakostas, V., Papadimitriou, E., Mesimeri, M., Gkarlaouni, Ch., Paradisopoulou, P., 2015. The 2014 Kefalonia doublet (Mw6.1 and Mw6.0) central Ionian Islands, Greece: seismotectonic implications along the Kefalonia transform fault zone. Acta Geophys. 63, 1–16. https://doi.org/10.2478/s11600-014-0227-4.

Kiratzi, A., Langston, C., 1991. Moment tensor inversion of the 1983 January 17 Kefallinia event of Ionian islands (Greece). Geophys. J. Int. 105, 529–538.

Lekkas, E.L, Mavroulis, S.D., 2015. Earthquake environmental effects and ESI 2007 seismic intensities of the early 2014 Cephalonia (Ionian Sea, western Greece) earthquakes (January 26 and February 3, Mw 6.0). Nat. Hazards, 78, 1517-1544.

Louvari, E., Kiratzi, A.A., Papazachos, B.C., 1999. The Cephalonia transform Fault and its extension to western Lefkada Island (Greece). Tectonophysics 308, 223–236.

Marinatos, S. N., 1960. Helice: A submerged town of classical Greece, Archaeology 13, 186–193.

Marinou, A., Ganas, A., Papazissi, K., Paradissis, D., 2015. Strain patterns along the Kaparelli–Asopos rift (central Greece) from campaign GPS data, Ann. Geophys. 58(2), S0219. https://doi.org/10.4401/ag-6418.

McKenzie, D., 1972. Active tectonics of the Mediterranean region. Geophys. J. Roy. Astron. Soc. 30, 109–185.

Morewood, N., C., Roberts, G., 1999. Lateral propagation of the surface trace of the South Alkyonides normal fault segment, central Greece: its impact on models of fault growth and displacement–length relationships, J. Struct. Geol. 6, 635-653. https://doi.org/10.1016/S0191-8141(99)00049.

Pantosti, D., De Martini, P., Koukouvelas, I., Stamatopoulos, L., Palyvos, N., Pucci, S., Lemeille, F., Pavlides, S., 2004. Palaeoseismological investigations of the Aigion Fault (Gulf of Corinth, Greece), Compt Rendus Geosci. 336, 335–342.

Papadimitriou, E. E., 1993. Focal mechanisms along the convex side of the Hellenic Arc. Boll. Geofis. Teor. Appl. 140, 401-426.

Papadimitriou, E., Karakostas, V., Mesimeri, M., Chouliaras, G., Kourouklas, Ch., 2017. The Mw6.5 17 November 2015 Lefkada (Greece) earthquake: structural interpretation by means of the aftershock analysis. Pure Appl. Geophys. 174, 3869–3888.

Papathanasiou, G., Valkanioti, S., Ganas, A., 2021. Spatial patterns, controlling factors, and characteristics of landslides triggered by strike-slip faulting earthquakes: case study of Lefkada island, Greece. Bull.Eng. Geol. Environ. 80, 3747-3765.

Papazachos, B. C., Mountrakis, D. M., Papazachos, C. B., Tranos, M. D., Karakaisis, G. F., Savvaidis, A. S., 2001. The faults which have caused the known major earthquakes in Greece and surrounding region between the 5th century BC and today. Proceedings of 2nd National Conference Anti-Seismic Engineering and Technical Seismology, 17–26, Technical Chamber of Greece, Thessaloniki, Greece.

Rondoyanni, Th., Mettos, A., Paschos, P., Georgiou, Ch., 2007. Neotectonic map of Greece, scale 1:100.000, Lefkada sheet. I.G.M.E., Athens.

Rondoyanni, Th., Sakellariou, M., Baskoutas, J., Christodoulou, N., 2012. Evaluation of active faulting and earthquake secondary effects in Lefkada Island, Ionian Sea, Greece: an overview. Nat. Haz. 61(2), 843-860.

Schwartz, D.P., 2018. Past and future rupture lengths in seismic source characterization – the long and short of it. Bull. seism. Soc. Am. 108, 2493–2520. https://doi.org/10.1785/0120160110.

Scordilis, E., Karakaisis, G.F., Karakostas, V., Panagiotopoulos, D.G., Comninakis, P.E., Papazachos, B.C., 1985. Evidence for Transform Faulting in the Ionian Sea: The Cephalonia Island Earthquake Sequence of 1983. Pure Appl. Geophys. 123, 388-397.

Stefatos, A., Papatheodorou, G., Ferentinos, G., Leeder, M., Collier, R., 2002. Seismic reflection imaging of active offshore faults in the Gulf of Corinth: their seismotectonic significance. Basin Res. 14, 487–502.

Underhill, J. R., 1989. Late Cenozoic deformation of the Hellenide foreland, western Greece. Geol. Soc. Am. Bull. 101, 613-634.

Valkaniotis, S., 2009. Correlation between neotectonic structures and seismicity in the broad area of Corinth Gulf (Central Greece) (Doctoral dissertation; in Greek). Aristotle University of Thessaloniki, Thessaloniki, Greece.

4 GIS map and database of geology and seismotectonics (Bedretto lab and Swiss Alps)

In this section, the maps and database of geology and seismotectonics of Switzerland that are used in the QGIS project are described.

Most of the official swisstopo geospatial data have become freely available in recent years. For a quick overview or creating maps they can be displayed in any standard GIS Program such as QGIS as WMS (Web Mapping Service; https://wms.geo.admin.ch/). However, for calculations based on the geodata, they can be downloaded (often in various file formats, including shapefiles, Geodatabase (.gdb), and GeoPackage (.gpkg).

4.1 Geological and tectonic map

The GeoCover (v3) vector data set is based on the published maps of the Geological Atlas of Switzerland 1:25 000, partly revised, and on compilations extracted from the most recent geological map material that is available (swisstopo, 2023a).

The GeoCover dataset includes detailed geologic and tectonic features as points, lines and polygons, describing the sedimentary and bedrock layers and units (Fig. 4.1).

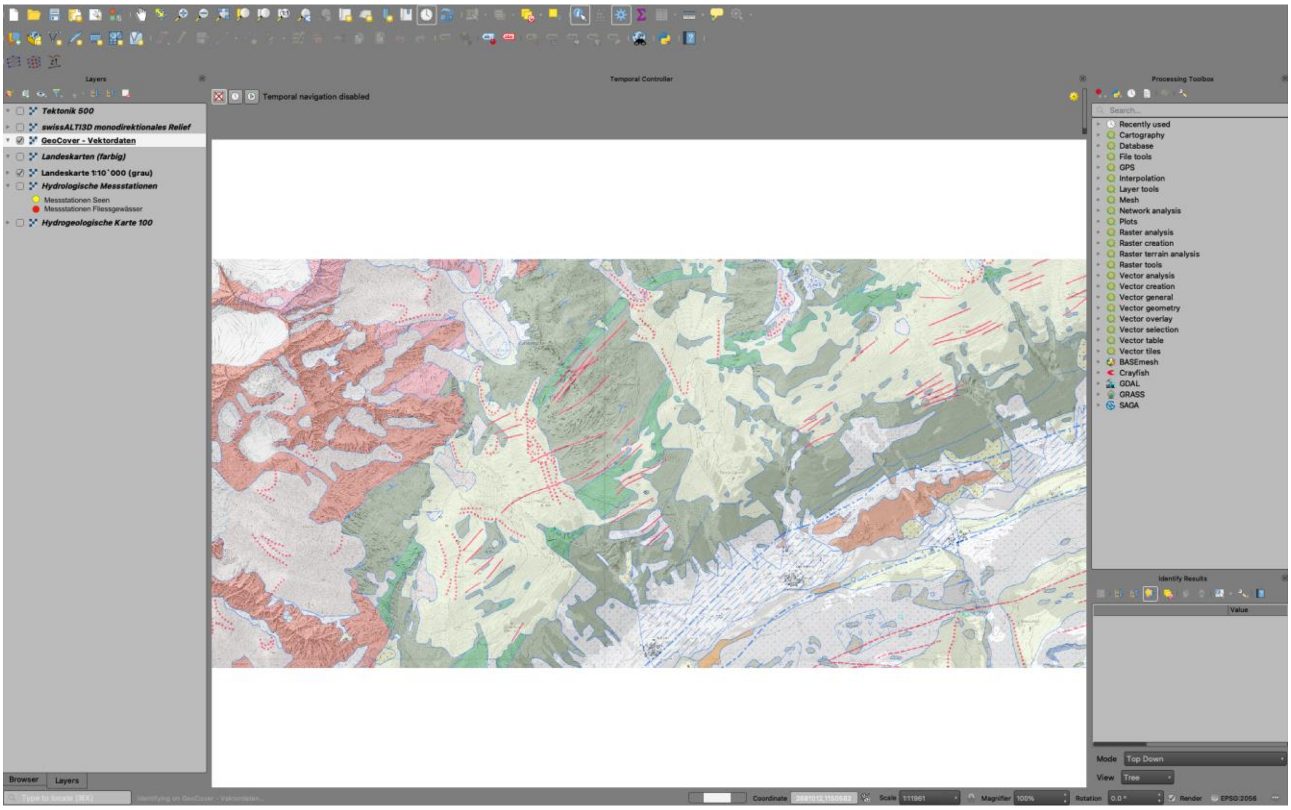

Figure 4.2: Extract of the GeoCover dataset (swisstopo) including lithologic and tectonic information

4.2 Large-scale tectonic map

The Tectonic map of Switzerland 1:500000 (swisstopo, 2023b) shows large-scale structural and tectonic units to give a better understanding of the geological structure of the Alps and their surroundings (Fig. 4.2).

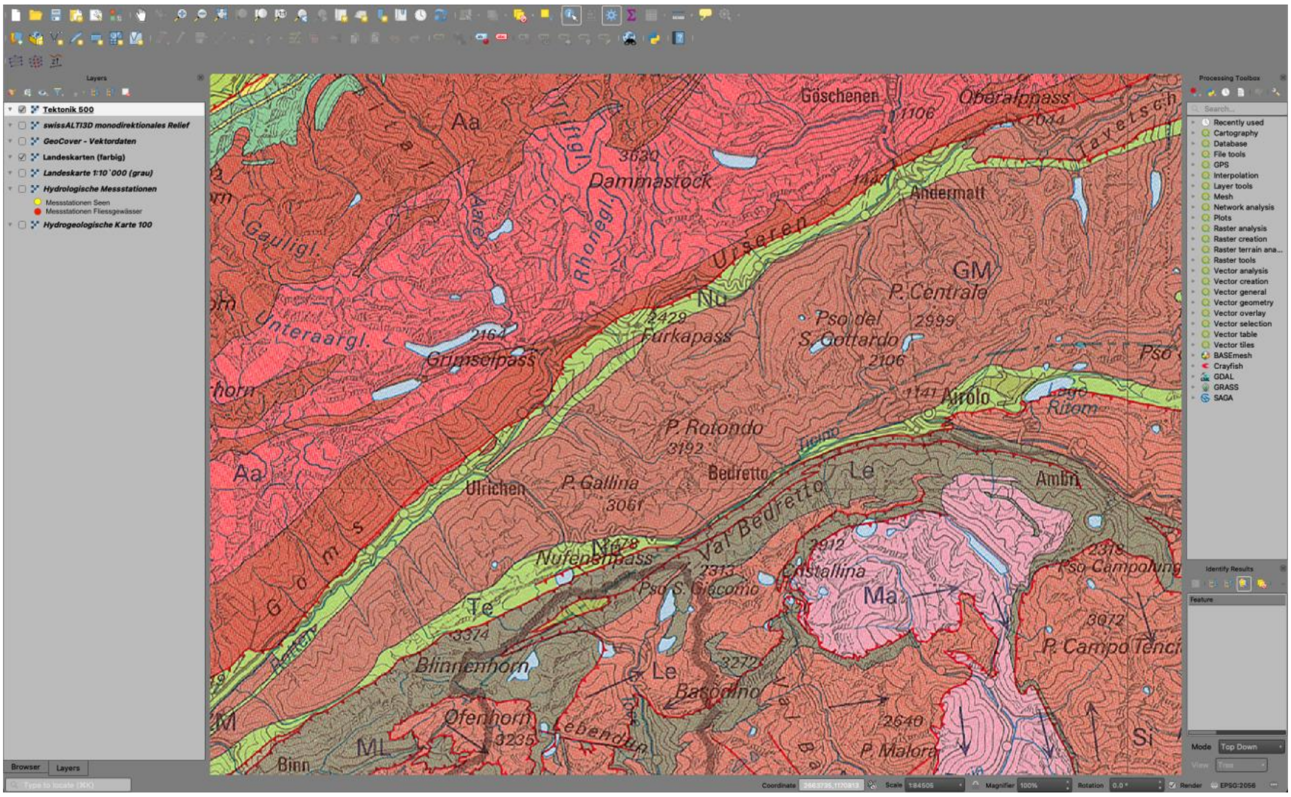

Figure 4.2: Extract of the “Tektonik 500” dataset (swisstopo) including lithologic and tectonic information

In the Bedretto tunnel, sampling locations are mainly described in tunnel meters (TM), where TM0 refers to the Tunnel entrance near the village of "Ronco". The sampling locations in the tunnel will be manually georeferenced based on the tunnel meters.

4.3 References

Swisstopo, 2023a. Geocover – Geological vetor datasets for better subsurface management. URL https://www.swisstopo.admin.ch/en/geodata/geology/maps/geocover.html (accessed 25.04.2023)

Swisstopo, 2023b. Tectonic Map of Switzerland 1:500000. URL https://data.geo.admin.ch/ch.swisstopo.geologie-tektonische_karte/ (accessed 25.04.2023)